RI-9175

RI 9175

Bureau of Mines Report of Investigations/1988

Critical Conditions for Ignition and Propagation of Mine Fires

By C. C. Hwang and C. D. Litton

UNITED STATES DEPARTMENT OF THE INTERIOR

Report of Investigations 9175

Critical Conditions for Ignition and Propagation of Mine Fires

By C. C. Hwang and C. D. Litton

UNITED STATES DEPARTMENT OF THE INTERIOR
Donald Paul Hodel, Secretary

BUREAU OF MINES
T S Ary, Director

Library of Congress Cataloging in Publication Data:

Hwang, C. C. (Charles C.)

Critical conditions for ignition and propagation of mine fires.

(Report of investigations ; 9175)
Bibliography: p. 18.
Supt. of Docs. no.: I 28.27:9175.
1. Mine fires--Prevention and control. I. Litton, C. D. (Charles D.). II. Title. III. Series: Report of investigations (United States. Bureau of Mines) ; 9175.

TN23.U43 [TN315] 622 s [622'.8] 88-600131

CONTENTS

ILLUSTRATIONS

ILLUSTRATIONS--Continued

TABLES

UNIT OF MEASURE ABBREVIATIONS USED IN THIS REPORT

°C	degree Celsius	MW	megawatt
cm	centimeter	m	meter
J/m^2	joule per square meter	m^2	square meter
K	kelvin	m/s	meter per second
kg	kilogram	m^2/s	square meter per second
kg/m^3	kilogram per cubic meter	min	minute
		pct	percent
kg/(m•s)	kilogram per meter per second	s	second
kg/s	kilogram per second	W/(m•°C)	watt per meter per degree Celsius
kJ/(g•°C)	kilojoule per gram per degree Celsius	W/m^2	watt per square meter
kJ/kg	kilojoule per kilogram	$W/(m^2•K)$	watt per square meter per kelvin
kJ/(kg•°C)	kilojoule per kilogram per degree Celsius	$W/(m^2•K^4)$	watt per square meter per kelvin to fourth power
kW	kilowatt		

CRITICAL CONDITIONS FOR IGNITION AND PROPAGATION OF MINE FIRES

By C. C. Hwang[1] and C. D. Litton[2]

ABSTRACT

The Bureau of Mines made time-dependent calculations to determine the size of a stationary source fire within a ventilated duct (or passageway) necessary to ignite a combustible duct liner. The objective of this work was to gain more understanding of what occurs in duct fires and to determine critical conditions for ignition and propagation of mine fires. Heat transfer to the combustible surface includes both convective and radiated components, while the heat is conducted into the combustible and reradiated to the surroundings. The combustible is assumed to ignite when the net heat transfer to its surface is sufficient to raise the surface temperature to some minimum temperature, defined as the ignition temperature. A nondimensional parameter, which characterizes the source-fire intensity in the presence of ventilation flow, emerges as a parameter for a criterion of the critical conditions. The results of these calculations indicated that the minimum fire size necessary for ignition increases with the ventilation rate and duct cross section. These results are compared with experimental results obtained from fires in a 0.8- by 0.8- by 11-m-long duct and a full-scale gallery (2.4- by 2.4- by 65-m). Agreement between the theory and the experiment is good.

[1]Mechanical engineer.
[2]Supervisory physical scientist.
Pittsburgh Research Center, Bureau of Mines, Pittsburgh, PA.

INTRODUCTION

Passageways lined with flammable materials constitute fire hazards. In an accidental fire, the materials can ignite and fire can propagate along the passageway. A typical example is fires in mine roadways. In previous studies of passageway (or duct) fires, the burning of both continuous fuel lining and discretely lined fuel elements (such as timber sets) was considered (1-7).[3] Those studies revealed an intimate coupling between the development of a fire and the forced ventilation flow in the duct. The severe fire hazards of excess fuel, heat, and smoke generation were direct consequences of this coupling. The studies also revealed the three-dimensional nature of the flow field, the importance of radiative contribution in fire propagation, and the effect of the strength of the ignition source on the subsequent growth of fire in the duct.

The probability for a combustible surface to ignite in the presence of some external heat flux depends upon the combustible properties of thermal conductivity, λ, and thermal diffusivity, α, and some minimum surface temperature for sustained flaming, T_{ig}, of the combustible material. Surface ignition is dependent upon the generation of sufficient fuel vapors from the combustible such that a flammable fuel-air mixture must have an autoignition temperature (or flashpoint) less than or equal to the surface temperature at ignition. In addition, secondary effects such as dilution of the pyrolysis products by forced convection and the formulation of surface char layers can affect the values obtained for T_{ig} under different conditions. In the present analysis, a single ignition temperature is assigned to one type of material (such as untreated Douglas fir).

A combination of the values of the source fire strength, $\dot{Q}_f$ and V_∞, which gives the fuel element, A_f, the T_{ig} at the end of a prescribed ignition time, τ_{ig}, is termed the critical conditions for duct-fire ignition. It is assumed that the term expressing the pyrolysis of the fuel element may be neglected in the conduction equation during the ignition time.

The objectives of this Bureau of Mines study are to gain more understanding of the energy transport taking place in duct fires in their initial transient period, and to determine the critical conditions for ignition and propagation under various fire environments. Specifically, calculations are made on the heating of fuel linings (or fuel elements) by a source fire in a ventilation duct. From these calculations, the size of a source fire within a ventilated duct necessary to ignite a combustible liner is determined. The results of computations are compared to the experimental results from the Bureau's fire tunnel (0.8- by 0.8-m cross section) and from a simulated mine gallery (Factory Mutual Research Corp., Norwood, MA, 2.4- by 2.4-m cross section) (7).

ANALYSIS

The configuration of a fuel element relative to the ventilated duct and a source fire is shown in figure 1. The A_f represents a segment of either continuous fuel lining (1-6) or timber sets (8). The source fire is treated as a flame sheet, (A), normal to the ventilation flow. It is assumed that the ventilation air enters the source fire at temperature T_∞, and velocity V_∞, and as a result of the combustion of fuel in the source fire at a rate of $\dot{Q}_f$ watts, the combustion products emerge with temperature T_g and a velocity V_g. The source fire loses heat by radiation from the exposed end surfaces with an effective emissivity, (ε_f). As seen in figure 1,

[3] Underlined numbers in parentheses refer to items in the list of references preceding the appendixes at the end of this report.

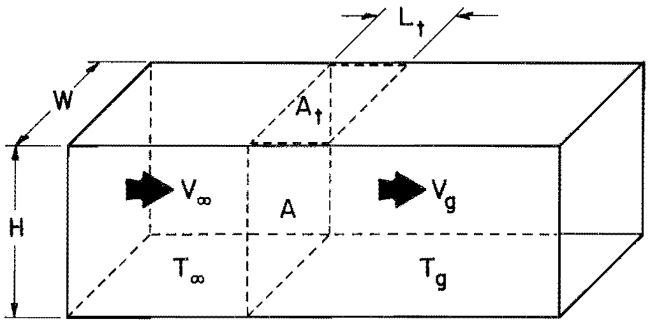

KEY
A = HW, flame sheet (source fire)
A_t = WL_t, timber supporting the ceiling

FIGURE 1.–Relative positions of flame and fuel-element in ventilated passageway.

the source fire is immediately upstream from the fuel element. The source fire may be the flame from burners (in experiment), timber fire, or a combination of these. It is believed that this fire-fuel configuration gives the A_t (or its two supporting members, constituting a timber set, not shown) the severest fire environment. This fire-fuel configuration can also apply to a continuous fuel lining.

HEAT CONDUCTION EQUATIONS FOR FUEL ELEMENTS

The heat conduction equation for the fuel elements is

$$\frac{\partial T_t}{\partial t} = \alpha_t \frac{\partial^2 T_t}{\partial y^2}, \qquad (1)$$

with boundary conditions

$$-\lambda \frac{\partial T_t}{\partial y} = h_t(T_g - T_t)$$

$$+ q''_{r,net}, \; y = 0, \; t > 0, \qquad (2)$$

$$y \to \infty, \; t > 0, \qquad (3)$$

$$T_t = T_\infty,$$

and initial condition

$$T_t = T_\infty, \; 0 < y < \infty, \; t = 0, \qquad (4)$$

where T is temperature, α is the thermal diffusivity, y is the distance from and normal to the fuel surface, λ is the thermal conductivity, h is the heat transfer coefficient, and $q''_{r,net}$ is the net radiative heat flux. The subscripts t, g, and ∞ denote timber (fuel element), gas, and condition upstream of source fire, respectively. It has been assumed that the fuel element is a semi-infinite solid. In the present analysis, the maximum time considered is $t_{max} \approx 60$ min. Therefore, the characteristic distance of heat penetration, ℓ, into the timber is $\ell = (\alpha_t \, t_{max})^{1/2} = 1.86 \times 10^{-2}$ m, which is about 40 pct of the thickness of the smallest timber used in the study. This calculation shows that the semi-infinite solid approximation for the timber is valid in the present analysis. It is also assumed that the heat transfer parallel to the solid surface is negligible compared with the heat transfer in the normal direction.

ENERGY CONSIDERATION FOR THE SOURCE FIRE

The gas temperature T_g in equation 2 is directly related to $\dot{Q}_f$ and V_∞. By taking a control volume around A in figure 1, the continuity equation and energy equation can be written as

$$\dot{m}_\infty + \dot{m}_f = \dot{m}_g, \qquad (5)$$

$$\dot{m}_\infty c_{p\infty} T_\infty + \dot{m}_f c_{pf} T_\infty + \dot{m}_f \Delta H$$

$$= \dot{m}_g c_{pg} T_g + 2A\varepsilon_f \sigma T_g^4, \qquad (6)$$

where $\dot{m}$ is mass flow rate, c_p is specific heat, ΔH is heat of reaction, A is the duct cross-sectional area, σ is Stefan-Boltzmann constant, and $\dot{Q}_f = \dot{m}_f \Delta H$. The subscripts f, g, and ∞ denote fuel, gas, and condition upstream of the source fire, respectively. It has been assumed that the gases involved are perfect gases. A common practice is to assume $c_{p\infty} = c_{pf} = c_{pg} = c_p$. If c_p is assumed constant, however, preliminary calculations show that the predicted T_g is progressively in error when T_g is higher than approximately 1,400 K (when $\dot{m}_f/\dot{m}_\infty \sim 0.03$, taking ΔH as 5.02×10^4 kJ/kg for CH_4). For this reason, c_p is taken as a linear function of T_g,

$$c_p = c_{p\infty}\,[1 + \beta(T_g - T_\infty)],$$
$$T_g < 2{,}100 \text{ K}. \qquad (7)$$

A procedure to determine the value of β is given in appendix A.

By defining $\theta = T_g/T_\infty$, and $\dot{Q}_f = \dot{m}_f\Delta H$, equations 5 through 7 can be reduced to

$$\theta^4 + a_1(\theta - 1) + a_2\theta(\theta - 1) = a_3, \qquad (8)$$

where $a_1 = c_{p\infty}\,(\dot{m}_\infty + \dot{Q}_f/\Delta H)/(2A\epsilon_f\sigma T_\infty{}^3)$,

$a_2 = \beta t_\infty a_1$,

and $a_3 = \dot{Q}_f/(2A\epsilon_f\sigma T_\infty{}^4)$.

The T_g (or equivalently, θ) emerging from the flame sheet is determined from equation 8. Once T_g is obtained, the gas velocity V_g can be determined from equation 5.

$$V_g = \rho_{g\infty}V_\infty/\rho_g + \dot{Q}_f/(\rho_g A\Delta H). \qquad (9)$$

CONVECTIVE HEAT TRANSFER COEFFICIENT

The convective heat transfer coefficient for the fuel element, h_f, appearing in equation 2 is calculated from

$$\frac{h_f L_f}{\lambda_f} = C\left(\frac{\rho_g V_g L_f}{\mu_g}\right)^m Pr^n, \qquad (10)$$

where C, m, and n are constants (for instance, see 9, p. 219), and Pr is the Prandtl number defined by $Pr = c_{pg}\,\mu_g/\lambda_g$. Equation 10 is intended for a timber with $L_f \times L_f$ cross section and with its axial length perpendicular to the ventilation flow. A similar expression can be used for a continuous fuel element.

RADIATIVE HEAT FLUX

The emission from a fire in general exhibits the characteristics of emission from a luminous as well as a nonluminous flame. Emission from a nonluminous flame is mainly from water vapor, carbon dioxide, and carbon monoxide, and quite an accurate estimate can be made. The emission from a luminous flame depends on the number of carbon particles present, which varies greatly with the conditions under which the combustion occurs. At present, the formation of carbon particles cannot be predicted under duct-fire conditions. As a result, it is not possible to calculate the flame radiation accurately. For this reason, various approximations to the radiative heat flux term $q''_{r,net}$ in equation 2 will be discussed in the analysis which follows.

Reradiation From Fuel Element Considered--Case 1

The term $q''_{r,net}$ appearing in equation 2 will be expressed (10, p. 687) as

$$q''_{r,net} = P\epsilon_f\sigma(T_g{}^4 - T_f{}^4), \qquad (11)$$

where P is an empirical factor which depends mainly on the fuel and on the size of the duct. This expression for $q''_{r,net}$ results in a nonlinear boundary condition for equation 2, and requires a numerical solution technique for solution to the heat conduction equation. The implicit Crank-Nicolson method combined with iterative steps (because of the $T_f{}^4$ term in the boundary condition) is employed for obtaining the solution.

Approximate Solution, Reradiation Neglected--Case 2

The term $q''_{r,net}$ in equation 2 can now be written as

$$q''_{r,net} = F\epsilon_f\sigma T_g{}^4, \qquad (12)$$

where F can be taken as the view factor from A to A_f (fig. 1). A justification for this approximation is that it results in a simplified boundary condition (and solution) for the problem, because the radiation term becomes a constant. In the section for results, the predicted critical conditions based on this boundary condition agree quite well with experiments.

The fuel surface temperature based on the boundary conditions (equation 2), with $q''_{r,net}$ given by equations 12 and 3 and initial condition (equation 4) is

$$T_{f,y=0} = T_\infty + (T_g - T_\infty + q''_{r,net}/h_f)\, G(t), \quad (13)$$

where $G(t) = 1 - [1 - \mathrm{erf}\{h_f(\alpha_f t)^{1/2}/\lambda_f\}]\exp(h^2\alpha_f t/\lambda_f^2)$.

A derivation of equation 13 is given in appendix C.

The critical conditions $T_{f,y=0} = T_{ig}$ for given value of τ_i can be calculated from equation 13. First, set $t = \tau_{ig}$, $T_{f,y=0} = T_{ig}$ in equation 13 and solve for T_g. In equation 13, h_f is still unknown, but can be calculated approximately by using $(\rho_\infty V_\infty)$ instead of $(\rho_g V_g)$ in equation 10. Once T_g is determined, $\dot{m}_f$ can be calculated from equation 6. The source-fire strength $\dot{Q}_f$ can be calculated from $\dot{Q}_f = \dot{m}_f \Delta H$. New values of $(\rho_g V_g)$ from equation 5 and h_f from equation 10 are now obtained, and the calculations are repeated until a convergence is obtained.

Pure Convection

This is a special case discussed above by setting $q''_{r,net} = 0$. By neglecting the radiative heat transfer and considering only the convective heat transfer, a higher value of T_g, than that when both heat transfer modes are retained, is required to reach T_{ig} for a given τ_{ig}. This solution, therefore, provides an upper bound for the flame temperature T_g in which a fuel element may be exposed. As expected, calculations for case 1 (purely numerical) and case 2 (analytical) agree when $q''_{r,net} = 0$.

PARAMETERS FOR THE SOURCE FIRE

The experimental studies reveal that the source fire strength $\dot{Q}_f$ and the ventilation air velocity V_∞ are the two major parameters which influence the development of passageway fires. A dimensionless parameter, $E = \dot{Q}_f/(\dot{m}_\infty c_{p\infty} T_\infty)$, which combines $\dot{Q}_f$ and V_∞, has been employed by Hwang (8) in an analysis on the effect of duct fire on the ventilation air velocity, and by Tewarson (7) to present his experimental data of full-scale fire tests. The parameter E can be shown to relate to other relevant parameters for the source fire. Dividing both sides of equation 6 by $\dot{m}_\infty c_{p\infty} T_\infty$ yields, after some algebraic manipulations,

$$E = (1 + \dot{m}_f/\dot{m}_\infty)[(1 + \beta\Delta T)(1 + \Delta T/T_\infty) - 1] + R(1 + \Delta T/T_\infty)^4 \quad (14)$$

where $\Delta T/T_\infty = (T_g - T_\infty)/T_\infty$,

and $R = 2A\varepsilon_g \sigma T_\infty^3/(\dot{m}_\infty c_{p\infty}) = 2\varepsilon_f \sigma T_\infty^3/(\rho_\infty c_{p\infty} V_\infty)$.

The approximate behavior of equation 14 for a normal mine-fire situation is desired. If the values of T_g up to $T_{ig} = 673$ K are considered, $0.1 < \Delta T/T_\infty < 1.26$. The maximum values of $\dot{m}_f/\dot{m}_\infty$ is 0.06 (corresponding to stoichiometric condition), and the values of $\beta\Delta T$ and R and $\beta\Delta T$ are at most 0.03 and 0.08, respectively. In appendix A, β is determined to be 0.0001961 K^{-1}. Therefore, $\beta\Delta T$ is one order of magnitude smaller than $\Delta T/T_\infty$, with $T_\infty = 298$ K. Under these conditions, the right-hand side of equation 14 becomes $\Delta T/T_\infty + R(1 + \Delta T/T_\infty)^4$, and for small value of $\Delta T/T_\infty$, say 0.2,

$$E \approx \Delta T/T_\infty, \quad (15)$$

that is, E varies linearly with $\Delta T/T_\infty$. The effect of the parameter R (effect of flame radiative transfer) becomes important as ΔT (or T_g) increases. From equation 14 the geometric scale factor (or cross-sectional area A) of the passageway appears only through $E = (\dot{Q}_f/c_{p\infty}T_\infty)/(V_\infty A)$ when E is plotted against $\Delta T/T_\infty$ with R as the parameter. This plot is shown in figure 2 along with the experimental data obtained from a simulated gallery (7). As predicted by equation 15, E varies linearly with $\Delta T/T_\infty$ for small values of $\Delta T/T_\infty$ (45° slope in log-log plots).

Figure 2 shows that the effect of R becomes increasingly larger as $\Delta T/T_\infty$ increases beyond 1.0. As E increases, the temperature change across the source fire ($\Delta T/T_\infty$) increases. As the value of R increases, $\Delta T/T_\infty$ decreases for a given value of E, indicating a shift from convective energy transfer to radiative transfer from the source fire. In general, the experimental data points fall under the curve for pure convective energy transfer (R = 0). The present analysis assumes zero heat loss to the contacting walls in the source fire zone, whereas some heat losses exist in the experiment. Therefore, the theoretical curves represent upper bounds for $\Delta T/T_\infty$.

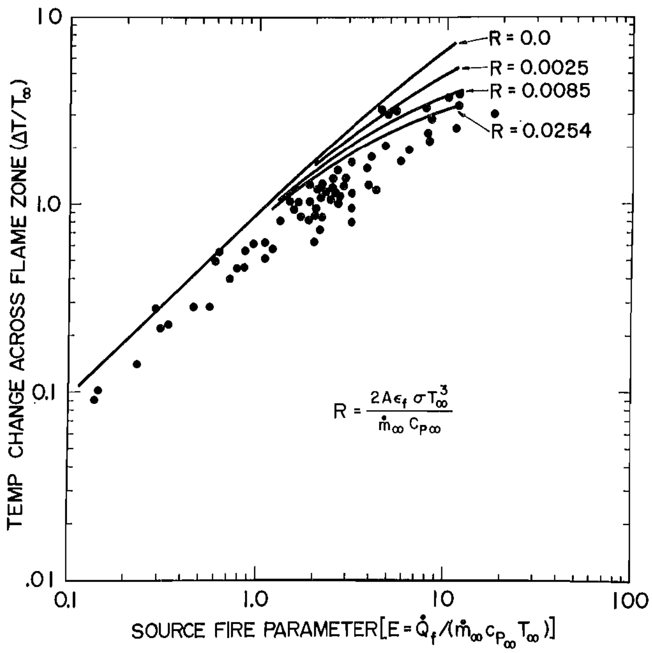

FIGURE 2.–Gas temperature rise across source fire versus source fire parameter E.

CRITERION FOR IGNITION

The critical condition for a steady passageway fire in the present formulation is defined as a combination of the values of $\dot{Q}_f$ and V_∞, which give a fuel element the ignition temperature T_{ig} at the end of a prescribed ignition time τ_{ig}. At the end of a finite value of τ_{ig}, the net heat transfer across the surface of the fuel-element must be greater or equal to zero; otherwise the surface cannot reach T_{ig}. From equations 2 and 11,

$$h_f(T_g - T_{ig}) + P\varepsilon_f\sigma(T_g^4 - T_{ig}^4) \geqslant 0,$$

or

$$T_g \geqslant T_{ig}, \text{ at } t = \tau_{ig} \tag{16}$$

which is the necessary condition for ignition.

The gas temperature T_g, or equivalently, the gas temperature rise across the source fire, $\Delta T = T_g - T_\infty$, is related to other parameters as given in equation 14. Equation 15 appears to hold for $\Delta T/T_\infty$ up to approximately 2 (fig. 2). By comparing equations 15 and 16, the necessary condition for duct-fire ignition is

$$E \geqslant (T_{ig} - T_\infty)/T_\infty, \text{ at } t = \tau_{ig}. \tag{17}$$

QUALITATIVE BEHAVIOR OF THE MODEL

A quantity that is relevant to the heating of a fuel-element is the time-integrated heat flux, q''_{tot}, into the fuel surface for the duration of the ignition time τ_{ig}, and is given by

$$q''_{tot} = -\int_0^{\tau_{ig}} \lambda_t \left.\frac{\partial T_t}{\partial y}\right|_{y=0} dt$$

$$= \lambda_t (T_{ig} - T_\infty) \left(\frac{\tau_{ig}}{\alpha_t}\right)^{1/2} \int_0^1 \left(-\frac{\partial \phi_t}{\partial \eta}\right)_{\eta=0} d\tau,$$

or

$$\frac{q''_{tot}}{\lambda_t (T_{ig} - T_\infty)} \left(\frac{\alpha_t}{\tau_{ig}}\right)^{1/2} = \int_0^1 \left(-\frac{\partial \phi_t}{\partial \eta}\right)_{\eta=0} d\tau, \quad (18)$$

where $\tau = t/\tau_{ig}$, $\eta = y/\ell = y/(\alpha_t \tau_{ig})^{1/2}$,

and $\phi_t = (T_t - T_\infty)/(T_{ig} - T_\infty)$.

Extensive computations are performed for ignition times τ_{ig} = 1, 10, 30, and 60 min. The physical and thermal properties of the fuel element are given in table 1, and the ignition temperature, T_{ig}, for untreated fuel is taken as 400° C. Tables 2 and 3 list the results of computations for the exact solution (reradiation from the fuel element considered) for small and large ducts, respectively.

TABLE 1. - Relevant values used in computations

Constants[1]	
C	0.102
m	0.675
n	0.333
Heat of reduction (ΔH), kJ/kg	5.02×10^4
Length of a timber along axial direction of duct (L_t), m:	
Small duct	0.15
Large duct	0.45
Temperature upstream of flame zone (T_∞), K	298
Gas density upstream of flame zone ($\rho_{g\infty}$), kg/m^3	[2]1.177
Specific heat of gas upstream of flame zone ($c_{p\infty}$), kJ/kg·°C	[2]1.005
Thermal conductivity of gas (λ_g), W/m·°C	[3]0.0523
Viscosity of gas (M_g), kg/m·s	[3]3.332×10^{-5}
Density of timber (ρ_t), kg/m^3	[4]420
Thermal conductivity of timber (λ_t), W/m·°C	[4]0.11
Specific heat of timber (c_{pt}), kJ/kg·°C	[4]2.72
Temperature coefficient for specific heat (β), K^{-1}	[5]0.0001961
Stefan-Boltzmann constant (σ)	

[1]From Holman, (9, p. 219), used in equation 10.
[2]At 300 K.
[3]At 700 K.
[4]Fir wood at 23° C.
[5]Used in equation 7.

TABLE 2. - Results of computations, small duct (wood)

τ_{ig}, min	$P\varepsilon_t$	T_{ig}, K	$\dot{Q}_f$, kW	V_∞, m/s	T_g, K	$\Delta T/T_\infty$	$E = \dfrac{\dot{Q}_f}{\dot{m}_\infty c_{p\infty} T_\infty}$	q''_{tot}, J/m^2	$\dot{Q}_f \tau_{ig}$, J	$\dfrac{\sqrt{\alpha_t}}{\lambda_t (T_{ig} - T_\infty)} \dfrac{q''_{tot}}{\sqrt{\tau_{ig}}}$
WITH DIFFERENT IGNITION TIMES										
1...	0	673	2,169	1.0	2,193	6.36	9.61	0.9363×10^6	0.1301×10^9	0.915
	0		2,457	1.5	1,822	5.13	7.26	0.9428×10^6	0.1474×10^9	0.920
	0		2,975	2.5	1,479	3.96	5.27	0.9533×10^6	0.1785	0.931
	1.0		253	.5	800	1.68	2.24	0.1006×10^7	0.1515×10^8	0.983
			471	1.0	797	1.67	2.09	0.1013×10^7	0.2826×10^8	0.989
			686	1.5	793	1.66	2.03	0.1016×10^7	0.4116	0.992
			1,109	2.5	787	1.64	1.97	0.1020×10^7	0.6654	0.996
10..	0		563	.5	1,426	3.79	4.99	0.3022×10^7	0.3376×10^9	0.993
			785	1.0	1,129	2.79	3.48	0.3085×10^7	0.4708	0.953
			990	1.5	1,013	2.40	2.93		0.594	
			1,370	2.5	904	2.03	2.43		0.822	
			201	.5	714	1.40	1.78	0.3447×10^7	0.1203×10^9	1.065
			380	1.0	713	1.39	1.68	0.3456×10^7	0.228	1.067
			560	1.5	712	1.39	1.65	0.3474×10^7	0.336	1.073
			915	2.5	710	1.38	1.62	0.3484×10^7	0.549×10^9	1.075
30..	0		371	.5	1,091	2.66	3.29	0.5367×10^7	0.668×10^9	0.956
			566	1.0	922	2.09	2.51	0.5514×10^7	1.0195×10^9	0.931
			751	1.5	857	1.87	2.22		1.351	
			1,107	2.5	798	1.68	1.96		1.992	
	1.0		190	.5	696	1.34	1.68	0.6108×10^7	0.342×10^9	1.090
			363	1.0	696	1.34	1.61	0.6140×10^7	0.653×10^9	1.095
			534	1.5	695	1.33	1.58	0.6140×10^7	0.961×10^9	1.095
			877	2.5	694	1.33	1.56	0.6163×10^7	0.158×10^{10}	1.099
60..	0		302	.5	958	2.22	2.67	0.7740×10^7	0.1086×10^{10}	0.976
			486	1.0	842	1.83	2.15	0.7974×10^7	0.1750	1.005
			664	1.5	798	1.68	1.96	0.8119×10^7	0.2389	1.023
			1,011	2.5	758	1.54	1.79	0.8305×10^7	0.3640×10^{10}	1.046
	1.0		186	.5	689	1.31	1.65	0.8737×10^7	0.670×10^9	1.101
			525	1.5	689	1.31	1.55	0.8789×10^7	1.89×10^9	1.108
			860	2.5	689	1.31	1.52	0.8783×10^7	3.10×10^9	0.614
WITH DIFFERENT RADIATION TRANSFER COEFFICIENTS										
10..	0.1	673	330	0.5	913	2.07	2.93	0.3105×10^7	0.198×10^9	0.960
	.3		245	.5	788	1.64	2.17	0.3208×10^7	0.147×10^9	0.991
	.5		221	.5	749	1.51	1.96	0.3306×10^7	0.133×10^9	1.021
WITH DIFFERENT IGNITION TEMPERATURES										
10..	0	773	748	0.5	1,720	4.77	6.63		0.4490×10^9	
10..	0	873	949	.5	2,010	5.75	8.41		0.5694×10^9	
10..	0	973	1,165	.5	2,297	6.71	10.33		0.6991×10^9	

ρ_t = 420 kg/m^3, λ_t = 0.11 W/mK, c_p = 2,720 (J/kg/K),
α_t = 9.63 × 10^{-8} m^2/s, T_{ig} = 673 K (if not stated), A = 0.64 m^2.

TABLE 3. - Results of computations, large duct (wood)

τ_{ig}, min	$P\varepsilon_t$	T_{ig}, K	$\dot{Q}_f$, kW	V_∞, m/s	T_g, K	$\Delta T/T_\infty$	$E = \dfrac{\dot{Q}_f}{\dot{m}_\infty c_{p\infty} T_\infty}$	q''_{tot}, J/m^2	$\dot{Q}_f \tau_{ig}$, J	$\dfrac{\sqrt{\alpha_t}}{\lambda_t (T_{ig} - T_\infty)} \dfrac{q''_{tot}}{\sqrt{\tau_{ig}}}$
WITH DIFFERENT IGNITION TIMES										
1...	0	673	32,030	1.5	2,324	6.80	10.52	0.9346×10^6	0.1922×10^{10}	0.913
	0		37,310	.5	1,840	5.17	7.35	0.9424×10^6	0.2238	0.920
	0		42,090	3.5	1,596	4.36	5.92		0.2525	
	1.0		2,290	.5	803	1.69	2.26	0.1007×10^7	0.1374×10^9	0.983
			4,270	1.0	800	1.68	2.10	0.1009×10^7	0.2562	0.985
			6,230	1.5	797	1.67	2.05	0.1010×10^7	0.3738	0.986
			10,110	2.5	793	1.66	1.99	0.1014×10^7	0.6066	0.991
10..	0		7,003	.5	1,765	4.92	6.90	0.2986×10^7	0.4202×10^{10}	0.922
			9,236	1.0	1,343	3.51	4.55	0.3035×10^7	0.5541×10^{10}	0.936
			11,230	1.5	1,173	2.93	3.69		0.6740×10^{10}	
			14,920	2.5	1,016	2.41	2.94		0.8952×10^{10}	
			18,400	3.5	940	2.15	2.59		1.104×10^{10}	
	1.0		1,810	.5	715	1.40	1.78	0.3442×10^7	0.1086×10^{10}	1.063
			3,440	1.0	715	1.40	1.69	0.3455×10^7	0.2064	1.067
			5,060	1.5	714	1.39	1.66	0.3461×10^7	0.3036	1.069
			8,290	2.5	712	1.39	1.63	0.3474×10^7	0.4974	1.072
30..	0		4,327	.5	1,287	3.32	4.26	0.5257×10^7	0.7789×10^{10}	0.940
			6,226	1.0	1,043	2.50	3.07	0.5399×10^7	1.121×10^{10}	0.963
			7,980	1.5	946	2.18	2.62		1.436×10^{10}	
			11,320	2.5	859	1.99	2.23		2.073×10^{10}	
	1.0		1,715	.5	697	1.34	1.69	0.6110×10^7	0.3087×10^{10}	1.090
			3,270	1.0	697	1.34	1.61	0.6123×10^7	0.5886	1.089
			4,810	1.5	695	1.33	1.58	0.6117×10^7	0.8658	1.090
			7,910	2.5	695	1.33	1.56	0.6141×10^7	1.424	1.095
WITH DIFFERENT RADIATION TRANSFER COEFFICIENTS										
10..	0.1	673	7,500	1.5	882	1.96	2.46	0.3138×10^7	0.450×10^{10}	0.969
	.3		6,000	1.5	781	1.62	1.97	0.3254×10^7	0.360	1.005
	.5		5,500	1.5	746	1.50	1.81	0.3333×10^7	0.330	1.030
WITH DIFFERENT IGNITION TEMPERATURES										
10..	0.1	773	8,480	1.5	982	2.39	2.78	0.4028×10^7	0.5088×10^{10}	1.244
10..	.1	873	9,800	1.5	1,075	2.61	3.22	0.4945×10^7	0.5880×10^{10}	0.993
10..	.1	973	11,900	1.5	1,170	2.42	3.67	0.5958×10^7	0.6714×10^{10}	1.019
10..	0	973	22,706	1.5	1,857	5.23	7.46		1.362×10^{10}	
10..	0	873	18,632	1.5	1,631	4.47	6.12		1.118×10^{10}	
10..	0	773	14,809	1.5	1,402	3.71	4.86		8.885×10^9	

ρ_t = 420 kg/m^3, λ_t = 0.11 W/mK, c_p = 2,720 (J/kg/K),
α_t = 9.63 × 10^{-8} m^2/s, T_{ig} = 673 K (if not stated), A = 5.75 m^2.

The right-hand side of equation 18 is found to be a function of E independent of the duct size, ignition time, and radiation transfer coefficient (fig. 3). All the computed results for $T_{ig} = 673$ K are included in figure 3. The asymptotic value of E for which the ordinate parameter becomes large is approximately 1.5 for $T_{ig} = 673$ K. (According to equation 17, the value is 1.26). The ordinate parameter appears to approach an asymptotic value (minimum) as E becomes large (or $\Delta T = T_g - T_\infty$ becomes large) as seen from equation 15. As T_g increases, the fuel surface heat flux becomes more constant with respect to time. This can be seen from equations 2 and 11, with T_f varying from T_∞ to T_{ig} and T_g on the order of 2,000 K. The solution of equation 1 with a constant surface heat flux q''_o is (9, p. 104)

$$T_{f,y=0} - T_\infty = (q''_o/\lambda_f)(4\alpha_f t/\pi)^{1/2}. \tag{19}$$

The value of q''_o can be determined by substituting $t = \tau_{ig}$ and $T_{f,y=0} = T_{ig}$ to yield

$$\frac{q''_{tot}}{\lambda_f(T_{ig} - T_\infty)}\left(\frac{\alpha_f}{\tau_{ig}}\right)^{1/2} = \left(\frac{\pi}{4}\right)^{1/2} = 0.886. \tag{20}$$

This asymptotic value for the nondimensional time integrated heat flux can be interpreted as the minimum value for fuel surface ignition.

Qualitatively, the model predicts that as $\tau_{ig} \to \infty$, $T_g \to T_{ig}$. From equations 15 and 16, as these limits are approached, $E \to E_{min}$ and $q''_i \to q''_{min}$, where $q''_{min} = h_f(T_{ig} - T_\infty) + P\varepsilon_f\sigma(T_{ig}^4 - T_\infty^4)$, and $E_{min} = (T_{ig} - T_\infty)/T_\infty$. The quantity q''_i is the initial heat flux for the critical condition given by

$$q''_i = h_f(T_g - T_\infty) + P\varepsilon_f\sigma(T_g^4 - T_\infty^4). \tag{21}$$

A simple expression which has the correct limitimg forms is plotted in figure 4, for all of the model calculations at $P\varepsilon_f$

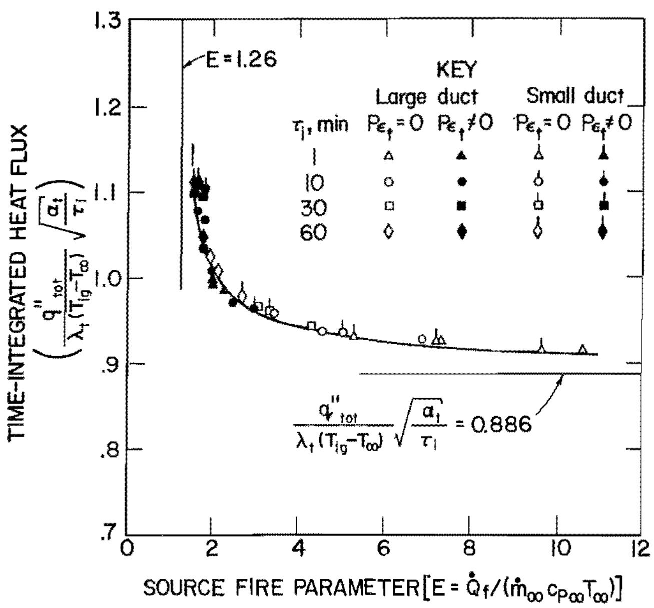

FIGURE 3.–Time-integrated heat flux as function of E.

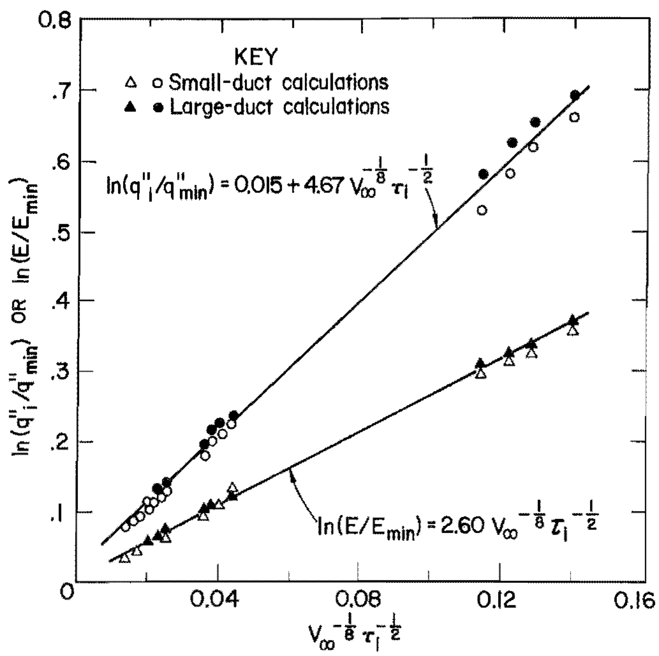

FIGURE 4.–Initial heat flux for critical conditions, q'_i, correlated with V_∞ and τ_i.

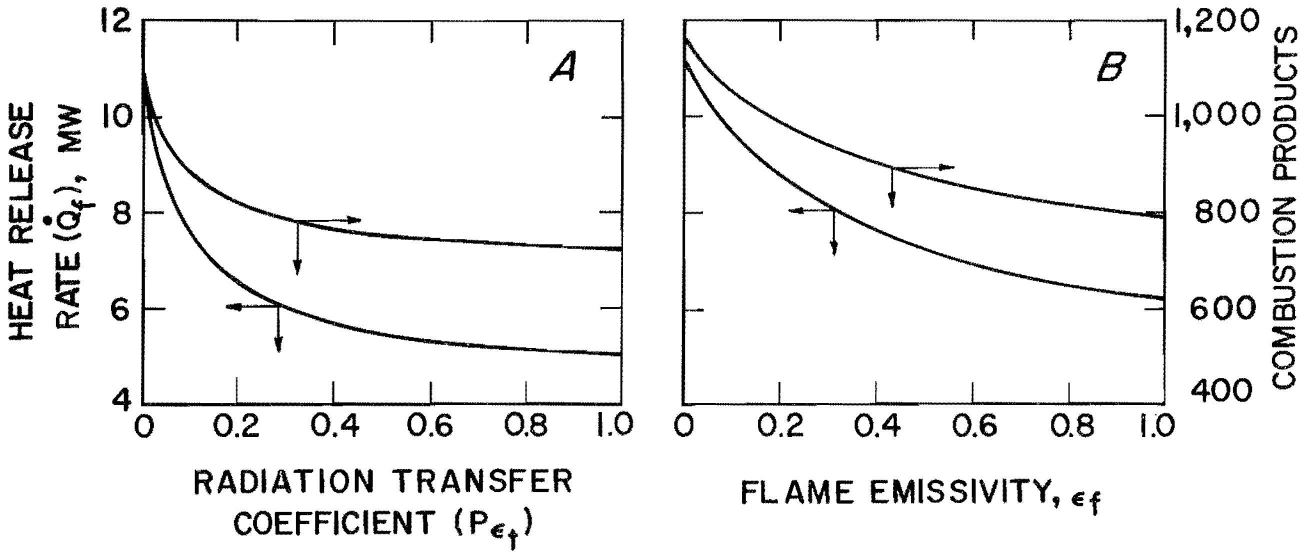

FIGURE 5.–Variations of T_g and $\dot{Q}_f$ at critical conditions as functions of P_{ϵ_t} and ϵ_f.

= 1.0 (radiation dominated heat transfer). The utility of this representation is demonstrated in the later section.

COMPARISON OF SOME SOLUTIONS

The values of $\dot{Q}_f$, T_g, and E at the critical conditions are calculated for given values of T_{ig}, V_∞, and τ_{ig}. In the present analysis, T_{ig} for untreated timber is taken as 400° C, the ignition time τ_{ig} is taken to be 1, 10, 30, and 60 min, and V_∞ is varied from 0.5 to 3.5 m/s.

Typical variations of T_g, and of $\dot{Q}_f$, as functions of $P\varepsilon_t$ (case 1) and ε_f (case 2) are shown in figure 5. It is seen that T_g is highest (upper bound) for pure convection ($P\varepsilon_t$ = 0, or ε_f = 0) and lowest (lower bound) for convection plus maximum radiation ($P\varepsilon_t$ = 1.0, or ε_f = 1.0). The concept of upper- and lower-bounds is extremely useful in this type of analysis, as it allows various fire scenarios to be encompassed with relatively small computational efforts. At the same time it allows comparison of the results of calculations to wide ranges of experimental variables.

The fraction of the radiative contributions to the total heat input to the fuel element, q''_r/q''_{tot}, as functions of $P\varepsilon_t$ and ε_f is shown in figure 6. The value of q''_r/q''_{tot} for ε_f = 1.0 (case 2) corresponds to the value for $P\varepsilon_t \approx 0.2$ (case 1). For $P\varepsilon_t$ = 1.0 the heat input to the fuel element is 90 pct radiation. Therefore, care must be taken in comparing the results of case 1 and case 2. Although both case 1 and case 2 can predict the critical conditions, the results of computations from case 1 will be used in the following presentation.

AVAILABLE EXPERIMENTAL DATA

In recent years, major experimental work on timber-set fires in passageways was carried out at the Bureau's fire tunnel and at the Factory Mutual Research Corp. facilities (6-7). This experimental work is described to provide a proper perspective of the theoretical analysis that has been described in the previous section.

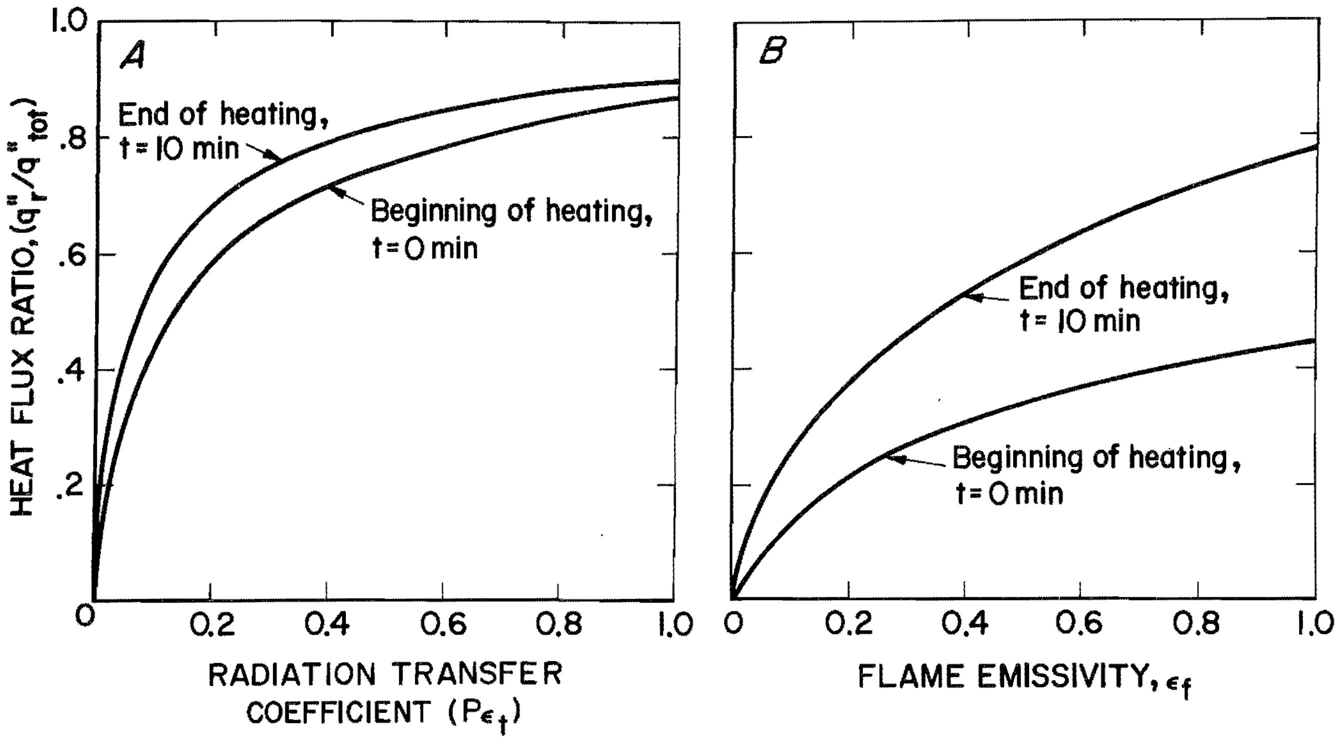

FIGURE 6.—Effects of $P\epsilon_t$ and ϵ_f on radiative contribution to heating of fuel element.

LARGE-SCALE TIMBER-SET FIRE TEST

The large-scale timber-set fire tests using a simulated mine gallery (located in West Gloucester, RI) were conducted by Factory Mutual Research Corp. (7). The objectives of the tests were to determine the conditions of fire propagation down a mine entry, which is lined with timber-sets at certain spacing, and to ascertain the hazards associated with such fires.

The gallery was a T-shaped structure with two passageways (drifts), each about 47 m long and about 2.4 by 2.4 m in cross-sectional area. The timbers were about 2.4 m long and approximately 0.15 by 0.15 m or 0.30 by 0.30 m in cross-sectional area. The timbers were used in the form of sets, each set consisting of two vertical timbers flush on the walls and one timber supported horizontally at the ceiling. The first set was located very close to the ignition source. Different timber loading densities were used in the tests, with timber loading density defined as the ratio of the total exposed surface area of all the timbers to the total surface area of the gallery walls and ceiling, where the timbers were located.

As an ignition source, a combination of premixed propane-air burners and wood boards was used. Two burners were used, one on each side wall flush with the wall. The boards were made from Douglas fir and each board was about 2.4 m long and about 0.05 by 0.02 m in cross-sectional area. The boards were placed vertically, between the floor and ceiling, about 0.15 m in front of each burner, in an array of 2 to 22 boards or total of 8 to 44 boards. The boards were separated by about 0.02 m along the length of the gallery and about 0.04 m toward the center of the gallery. Ignition of the boards by the burners was very uniform and repeatable, with peak intensity achieved within 60 to 120 s.

The ventilation air velocities ranged from about 0.5 to 3 m/s. The air entering the ignition source with a velocity V_∞ emerges from the source with a higher velocity V_g because of a large change in the gas temperature across the ignition source.

SMALL-SCALE TIMBER-SET FIRE TEST

The small-scale fire tests were conducted at the Bureau's fire tunnel. The tunnel consisted of a horizontal section about 11 m long and about 0.8 by 0.8 m in cross-sectional area. The objective of the test was to determine if scaling relationships could be developed that were capable of reliably projecting the small-scale test data to large-scale mine situations.

The timber sets were made from Douglas fir and were about 0.8 m long and 0.05 by 0.05 m in cross-sectional area. Similar to the arrangement in the large-scale gallery, each timber set consisted of two vertical timbers flush on the walls and one timber supported horizontally at the ceiling.

The ignition source was a pair of natural gas burners, one on each side of the tunnel. These burners produced opposing flame jets perpendicular to the ventilation air flow. The ventilation air velocity, V_∞, ranged from about 0.5 to 1.5 m/s.

TEST CONDITIONS

In the tests using either the simulated mine gallery or the small fire tunnel, the fire propagation and fire endurance of timber sets were studied by varying several parameters such as the (1) ventilation air velocity, (2) ignition sources, (3) size and spacing between timbers, (4) timber treatment, (5) horizontal and sloped passageways, and (6) bulkhead locations. Those tests revealed a close coupling among the ignition source, the ventilation air velocity, and the subsequent development of fire in a passageway. The temperature change across the ignition source was measured and correlated with other test variables. As expected, the fire intensity was higher for timber loading densities of 80- and 40-pct than for 20 pct.

COMPARISON OF MODEL WITH EXPERIMENT

In figure 7, the experimental values of E for the small fire tunnel is plotted as a function of time. Ignition occurs at t = 27 min in one case and t = 52 min in the other. Based on figure 7, the minimum critical value of E for ignition is approximately 1.3 for untreated timber sets. Equation 16 gives $E \geqslant 1.26$ with T_{ig} = 400° C.

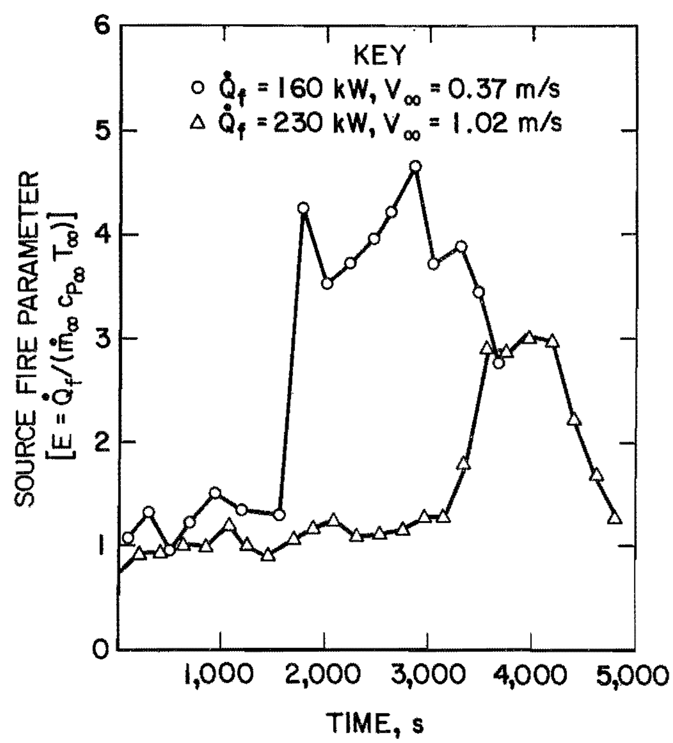

FIGURE 7.—E as function of time, small duct.

CRITERION FOR FIRE PROPAGATION

Figure 8 shows the ranges of E for fire propagation in the simulated mine gallery (7). The data indicate that E is dependent on the surface loading of timbers. In general, the critical value of E increases as the timber loading density decreases. On the theoretical ground, $\dot{Q}_f$ (or equivalency E) must increase to compensate for the heat losses to the unlined parts of the passageway as the loading density decreases. Tewarson (7) observes that a value of about 3 can be used as a minimum critical value of E for the initiation of sustained fire

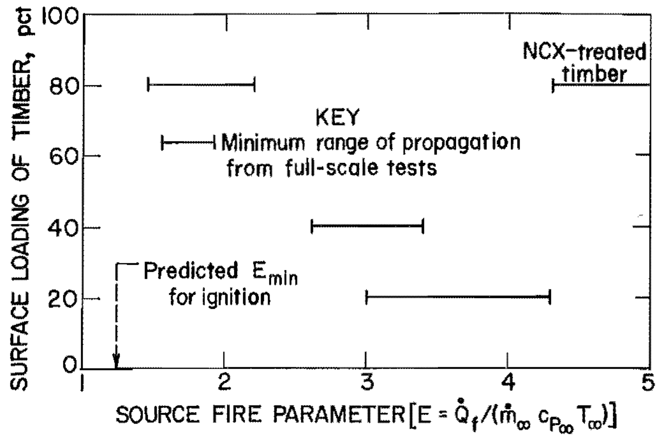

FIGURE 8.—Range of critical E for fire propagation in full-scale tests.

propagation for untreated timber sets. It will be seen later that the critical value of E is also a function of V_∞.

IGNITION TIME

The fire intensity parameter, E, is a coupling parameter that affects the heat transfer to the fuel element through equation 2. In order to relate the fire scenario to a fuel element, other parameters must be specified in addition to E, or $E = E\ (V_\infty,\ \tau_{ig},\ P\varepsilon_t,\ A,\ \alpha_t,\ \lambda_t,\ T_{ig})$. Calculations show that the parameters α_t and λ_t may be included in T_{ig}. The cross-sectional area, A, has small effects on E. The ignition time will be estimated from the experiments, in which T_{ig} is approximately constant. The experimental data from the simulated gallery (7) are plotted using $E - V_\infty$, coordinates in figure 9, along with the computed critical conditions. This set of data demarcates sustained fires from decaying fires, and it is seen that an ignition time of 10 min encompasses the upper bound for T_g ($P\varepsilon_t$ = 0.) and the lower bound for T_g ($P\varepsilon_t$ = 1.0). Figure 9 shows that the critical E is dependent on V_∞, especially for the case of pure convection. Similar plots for the experimental data from the small fire tunnel are shown in figure 10. This set of data is appropriate for ignition criterion, and an ignition time is approximately 60 min.

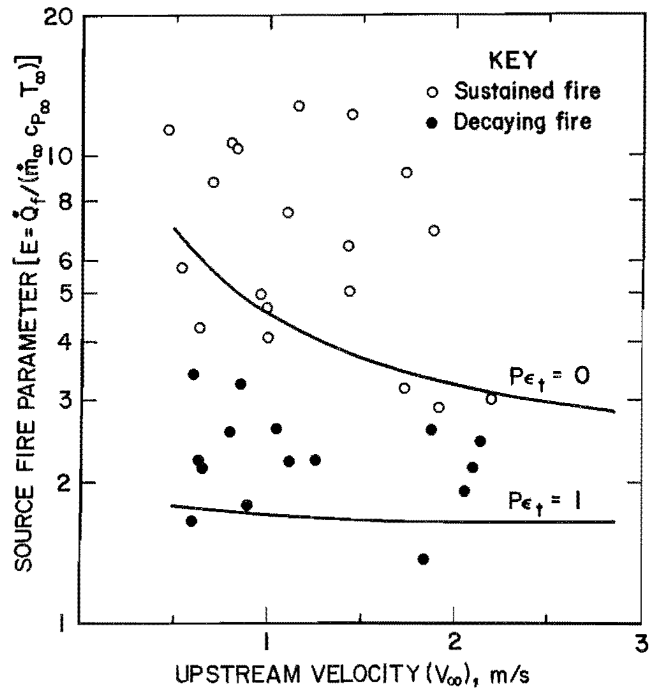

FIGURE 9.—E versus ventilation air velocity, simulated gallery experiments.

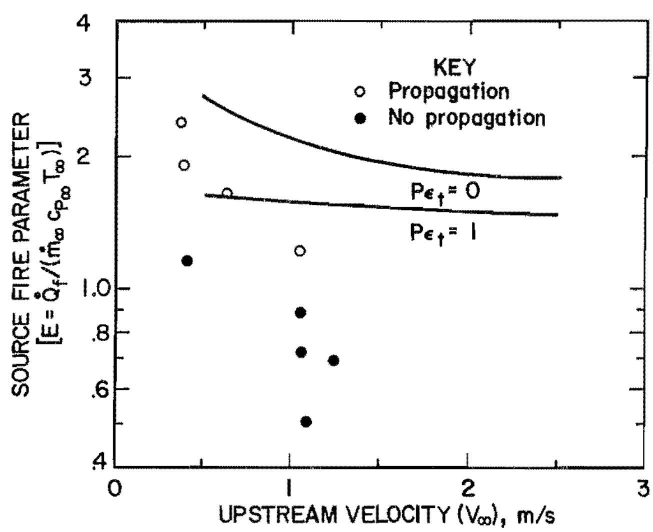

FIGURE 10.—E versus ventilation air velocity, small fire tunnel experiments.

EFFECT OF TIMBER TREATMENT ON FIRE PROPAGATION

Tewarson (7) observes that the minimum critical value of E for the initiation of sustained fire propagation for treated timber sets is approximately 5. Figure 8 shows the values of E for treated timber as well as untreated timbers. The test data (7) indicate that the treatment enhances surface charring and retention of carbon on the timber surface. It is also reported that the gas temperature for sustained piloted ignition is 773 K for NCX-treated Douglas fir, while the corresponding gas temperature for untreated Douglas fir is 660 K.

Based on the experimental observations and some preliminary calculations, it appears reasonable to use the ignition temperature as a parameter to model the effect of timber treatment on the propagation of duct fires. Figure 11 illustrates the effect of the timber ignition temperature, T_{ig}, on the critical value of E. The experimental data from the simulated gallery are also shown in figure 11. In the foregoing computations, variations in the physical properties, such as the timber density, ρ_t, thermal conductivity, λ_t, and specific heat, c_{pt}, are neglected; only the variation in T_{ig} has been considered. Figure 11 shows that the value of E ranges from 2.5 to 5.0 for an ignition temperature of 800 K.

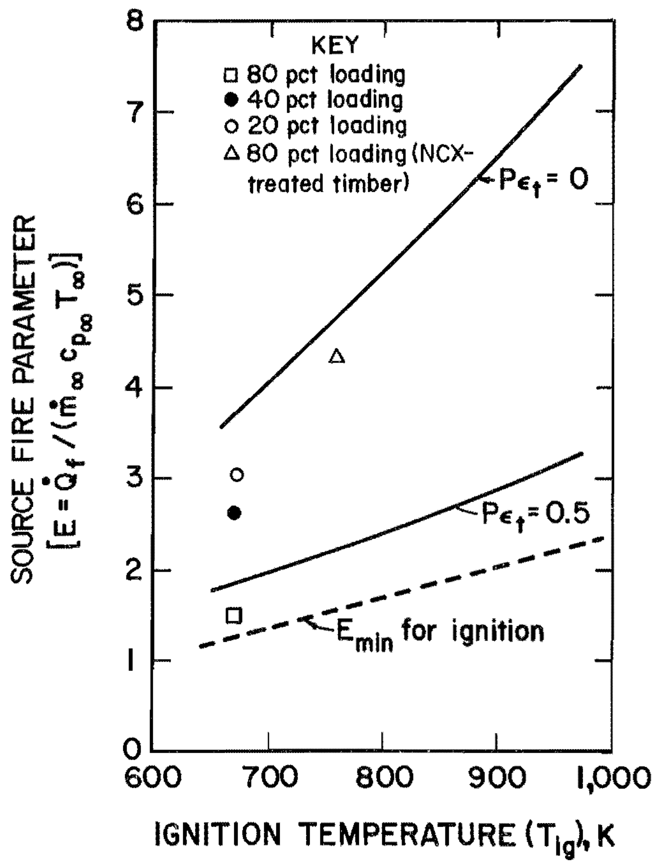

FIGURE 11.—Effect of ignition temperature on source-fire parameter E.

DATA RELEVANT TO q''_i

Figure 12 compares the results of ignition times with incident heat flux from experiments conducted in a small-scale combustibility apparatus (11-12) with the ignition time-incident flux correlation from the model calculations (fig. 4). In the experiments, the heat flux to the material surface was due to radiant heaters. Fourteen combustible materials were tested in this series of experiments, and although all the data are not shown, each combustible showed a linear correlation similar to that of figure 12, except for variations in the slope of the curves. It is felt that the different slopes reflect the ease with which the combustible is ignited and further, that these slopes are controlled by the factor $\alpha^{1/2}/\lambda$ for different materials, which should be expected on the basis of equation 19. In fact, a detailed look at the slopes of the three combustibles of figure 12, red oak, conveyor belt, and Douglas fir, show respective values for the slopes of 4.3, 5.2, and 5.7. These slopes appear to correlate well with the respective $\alpha^{1/2}/\lambda$ values of 1.95, 2.43, and 2.65.

The initial heat flux, q''_i defined by equation 21 and the heat flux, q''_f, when the timber surface temperature reaches the ignition temperature, $T_t = T_{max}$,

$$q''_f = h_t (T_g - T_{max}) + P\varepsilon_t \sigma (T_g^4 - T_{max}^4), \qquad (22)$$

are the characteristic quantities of the source fire-timber system. These quantities are found to be useful for the quick estimate of certain quantities in the system without invoking the exact (numerical) solution. The following examples show the utility of this procedure.

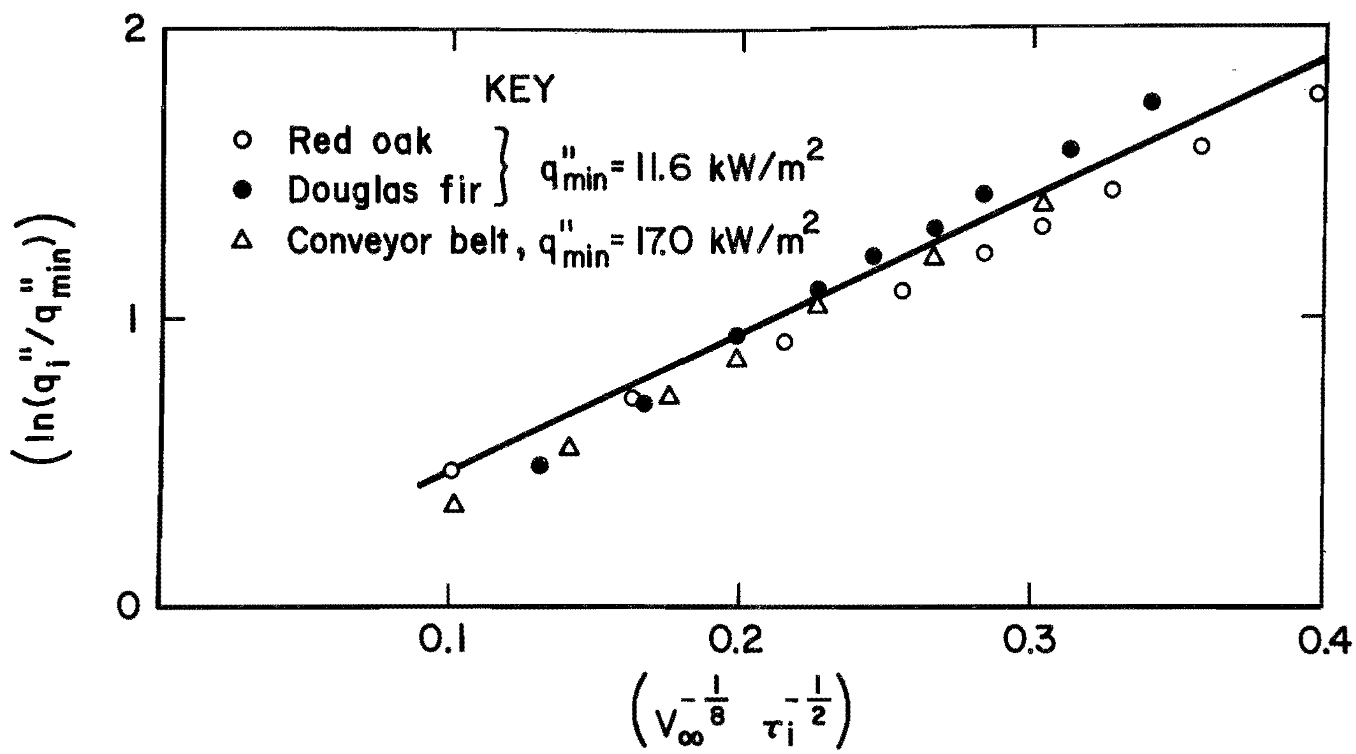

FIGURE 12.–Comparison of correlation in figure 4 with data from combustibility experiments.

EXAMPLE 1

Take the case of τ_{ig} = 30 min, V_∞ = 0.5 m/s, $P\varepsilon_t$ = 1.0. τ_{ig} will be calculated.

$$T_g = 697 \text{ K}$$

(table 2, or solving equation 8),

$$h_t = 4.052 \text{ W/m}^2\cdot\text{K}$$

(from equation 10).

First, q_i'' is calculated by equation 21.

$$q_i'' = 4.052\ (697 - 298)$$

$$+ (1)(1)(5.6697 \times 10^{-8})$$

$$[(697)^4 - (298)^4]$$

$$= 14{,}551 \text{ W/m}^2.$$

If it is assumed that the timber is heated by a constant surface heat flux q_i'', equation 19 can be used to calculate the time, t_{min}, for the surface to reach $T_{t,y=0} = T_{ig}$.

$$t_{min} = \frac{\pi}{\alpha}\left[\frac{\lambda_t}{2q_o''}\ (T_{t,y=0} - T_\infty)\right]$$

$$= 65.55 \text{ s}.$$

Similarly, q_f'' = 1,847 W/m²

and

$$t_{max} = 4{,}068.4 \text{ s},$$

$$\tau_i = 1/2\ (T_{min} + T_{max}) = 2{,}067 \text{ s},$$

which is 15 pct higher than the exact solution.

In the case of τ_i = 1 min, V_∞ = 0.05 m/s is taken

then

$$T_g = 803.1 \text{ K and } h_t = 4.061 \text{ W/(m}^2\cdot\text{K)}$$

$$q_i'' = 25{,}177 \text{ W/m}^2,\ t_{min} = 21.9 \text{ s},$$

$$q_f'' = 12.482 \text{ W/m}^2,\ t_{max} = 89.1 \text{ s},$$

and τ_i = 55.5 s, which is 7 pct lower than the exact solution.

EXAMPLE 2

The temperature distributions for the conditions given in example 1 will be calculated. For a constant heat flux q_o'' at the surface, the temperature distribution is given by

$$T(y,t) - T_o$$

$$= \frac{2q_o''}{\lambda_t}\sqrt{\frac{\alpha_t t}{\pi}}\exp\left(\frac{-y^2}{4\alpha_t t}\right)$$

$$- \frac{q_o'' y}{\lambda_t}\left[1 - \operatorname{erf}\left(\frac{y}{2\sqrt{\alpha_t t}}\right)\right]. \quad (23)$$

Case 1

τ_i = 2,067 s

Equation 19 is employed to calculate q_o'', with $T_{t,y=0} = T_{ig}$,

$$q_o'' = \left(\frac{\pi}{\alpha_t}\,\frac{\lambda_t}{2t_i}\right)^{1/2}(T_{ig} - T_\infty)$$

$$= 0.2592\times10^4 \ \mathrm{W/m^2}.$$

The temperature distribution is calculated from equation 23 with $t = \tau_{ig}$ and q_o'' = 0.2592×10^4 W/m^2.

Case 2

For this case,

τ_{ig} = 55.5 s,

q_o'' = 0.1582×10^5 W/m^2.

Figure 13 shows the temperature distributions computed from equation 23 and a numerical analysis. In both cases, the temperature distributions calculated from equation 23 are lower (~5 pct) than that from the numerical analysis.

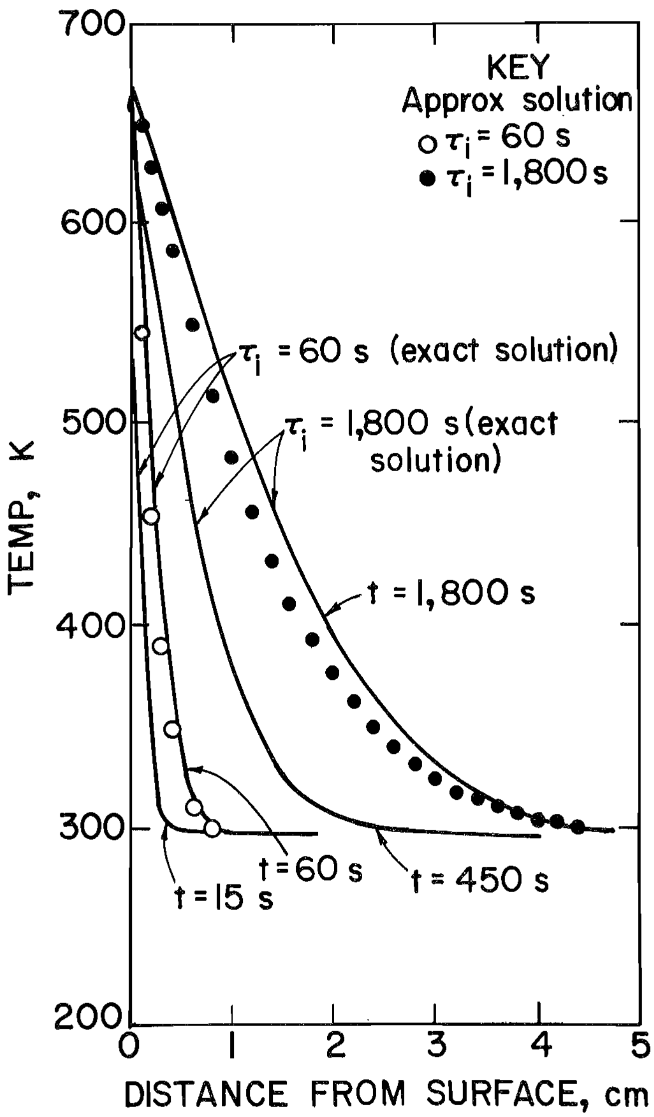

FIGURE 13.–Temperature distributions within timber, based on numerical and approximate solutions.

CONCLUSIONS

The conditions with which ignition and propagation of a fuel element occur for a given source-fire intensity are determined from a fire-fuel configuration which is believed to be the severest fire environment. By introducing the ignition time, τ_i, and the ignition temperature, T_{ig}, in the solution of heat conduction equation for the fuel element, it is possible to define the critical conditions for ignition and propagation of a passageway fire.

A nondimensional parameter, $E = \dot{Q}_f / (\dot{m}_\infty c_{p\infty} T_\infty)$, which characterizes the source-fire intensity in the presence of ventilation flow, emerges as a parameter for criterion of the critical conditions. It is found that for ignition of untreated timber, $E > 1.5$, for sustained fire propagation for untreated timber, $E > 3$, and for treated timber, $E > 5$. The timber treated with respect to fire resistance, and in turn high value of E, can be modeled by varying the timber ignition temperature. The time-integrated heat flux to the timber is successfully correlated with the parameter E, with appropriate scaling factors for the duct size and the ignition time.

The utility of the present analysis is twofold: First, in a generalized fire scenario within a ventilated passageway, the ignition of adjacent combustible surfaces depends upon the heat released by an initial source fire and the resultant heat flux to these adjacent combustible surfaces. The present analysis allows for the calculation of the required fire sizes for ignition within this generalized fire scenario as a function of passageway size, forced ventilation rate, and time. Under conditions of maximum radiation flux from the source fire, the calculated fire sizes represent minimum values for ignition and subsequent propagation. Secondly, the model calculations can be compared with experimental data for ignition and propagation under experimental conditions closely approximating the model conditions.

REFERENCES

1. Roberts, A. F., and G. Clough. The Propagation of Fires in Passages Lined With Flammable Materials. Combust. and Flame, v. 11, 1967, pp. 365-376.

2. ______. Model Studies of Heat Transfer in Mine Fires. Safety in Mines Research Establishment (Sheffield, England), SMRE Res. Rep. 247, 1967, 21 pp.

3. deRis, J. Duct Fires. Combust. Sci. and Technol., v. 2, 1970, pp. 239-258.

4. Edwards, J. C., H. E. Perlee, and R. F. Chaiken. Cylindrical Duct Fire Spread. BuMines RI 8258, 1977, 32 pp.

5. Lee, C. K., R. F. Chaiken, and J. M. Singer. Behavior of Model Tunnel Wood Fires in Ventilation Flow. BuMines RI 8450, 1980, 58 pp.

6. Lee, C. K., C. C. Hwang, J. M. Singer, and R. F. Chaiken. Influence of Passageway Fires on Ventilation Flows. Paper in Second International Mine Ventilation Congress (Reno, NV, Nov. 4-8, 1979). Pierre Mousset-Jones, ed., pp. 448-454.

7. Tewarson, A. Analysis of Full-Scale Timber Fire Tests in a Simulated Mine Gallery. Factory Mutual Research Corporation (Norwood, MA). Tech. Reps. J.I. OEON1.RA and J.I. OFON3.RA, June 1982, 55 pp.

8. Hwang, C. C., and R. F. Chaiken. Effect of Duct Fire on the Ventilation Air Velocity. BuMines RI 8311, 1978, 19 pp.

9. Holman, J. P. Heat Transfer. McGraw-Hill, 4th ed., 1979, 530 pp.

10. Eckert, E. R. G., and R. M. Drake, Jr. Analysis of Heat and Mass Transfer. McGraw-Hill, 1972, 806 pp.

11. Tewarson, A. Fire Hazard Evaluations of Mine Materials in a Small-Scale Combustibility Apparatus (contract J0395125 Factory Mutual Res. Corp.) BuMines OFR 77-83, 1982, 79 pp.; NTIS PB 83-196204.

12. Sapko, M. J., K. W. Mura, A. L. Furno, and J. M. Kuchta. Fire Resistance Test Method for Conveyor Belts. BuMines RI 8521, 1981, 27 pp.

APPENDIX A.--DETERMINATION OF FLAME TEMPERATURE

To determine the flame temperature, T_f, the continuity equation and energy equation across the flame zone can be written as

$$\dot{m}_\infty + \dot{m}_f = \dot{m}_g, \qquad \text{(A-1)}$$

$$\dot{m}_\infty c_{p\infty} T_\infty + \dot{m}_f c_{pf} T_\infty + \dot{m}_f \Delta H_c$$

$$= \dot{m}_g \, c_{p,prod} \, T_f. \qquad \text{(A-2)}$$

It is common practice to assume $c_{p\infty} = c_{pf} = c_{p,prod} = c_p$

If c_p is assumed constant, however, preliminary calculations show that the predicted T_f is progressively in error when T_f is higher than approximately 1,400 K ($\dot{m}_f/\dot{m}_\infty \approx 0.03$).

The following observation is made to see what must be done to overcome this difficulty. When the adiabatic flame temperature, T_f, of CH_4 burning in air is plotted against the equivalence ratio ϕ (or $\dot{m}_f/\dot{m}_\infty$), the curve exhibits a bell shape as shown in figure A-1. The adiabatic flame temperature, T_f, increases with $\dot{m}_f/\dot{m}_\infty$ until $\dot{m}_f/\dot{m}_\infty \approx 0.06$ (or $\phi \approx 1.0$); then T_f decreases with $\dot{m}_f/\dot{m}_\infty$. The correct procedure to determine the relationship of T_f and $\dot{m}_f/\dot{m}_\infty$ is to calculate the equilibrium composition associated with T_f for a given initial mixture $\dot{m}_f/\dot{m}_g$. The calculation, in general, involves an iterative procedure.

It is desirable to determine T_f approximately for a given value of $\dot{m}_f/\dot{m}_g$ without lengthy calculations. Equations A-1 and A-2 are rearranged to give

$$\frac{1 + \dfrac{\dot{m}_f}{\dot{m}_\infty}}{\dfrac{\dot{m}_f}{\dot{m}_\infty}} (T_f - T_\infty) = \frac{\Delta H}{c_p} \qquad \text{(A-3)}$$

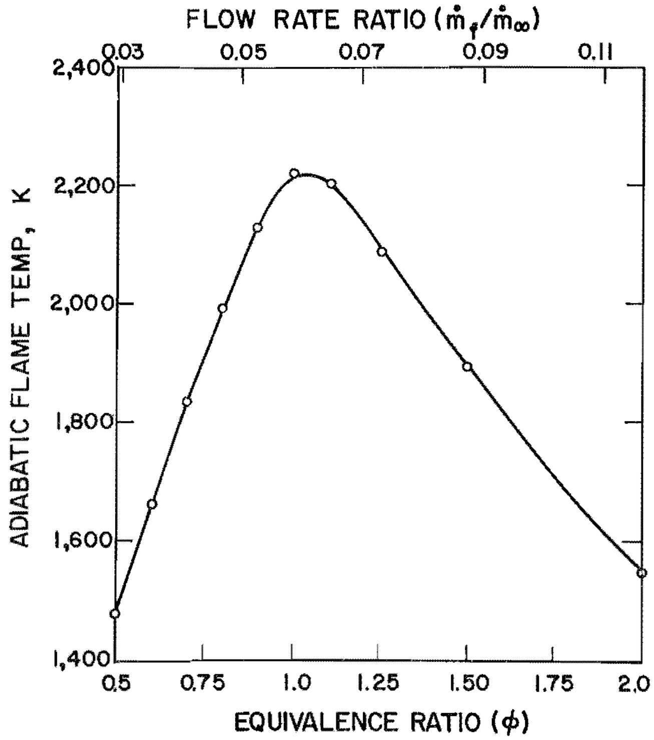

FIGURE A-1.--Adiabatic flame temperature for CH_4 burning in air.

The heat of reaction, ΔH, is taken as 5.02×10^4 kJ/kg. The specific heat is then calculated to yield the correct value of T_f for a given $\dot{m}_f/\dot{m}_\infty$ as in figure A-1. Table A-1 shows the results of this calculation. The dependence of c_p on T_f is shown more clearly in figure A-2. The specific heat of air is also plotted in figure A-2 to show that the specific heat of the combustion products of CH_4 may be approximated by the specific heat of air. As a first approximation

$$c_{p,prod} = c_{p,\infty} \left[1 + \beta \left(T_f - T_\infty\right)\right],$$

$$T_f < 2{,}100 \text{ K}. \qquad \text{(A-4)}$$

TABLE A-1. - c_p to yield correct T_f

T_f, K	$\dot{m}_f/\dot{m}_\infty$	c_p, kJ/g·°C	ϕ
1,477.......	0.0291	1.206	⩽1.0
1,662.......	0.0349	1.243	
1,835.......	0.0407	1.279	
1,994.......	0.0465	1.317	
2,131.......	0.0523	1.363	
2,223.......	0.0582	1.436	
2,208.......	0.0640	1.583	>1.0
2,094.......	0.0727	1.896	

The value of β used in the analysis is 0.0001961 K^{-1}, determined from figure A-2.

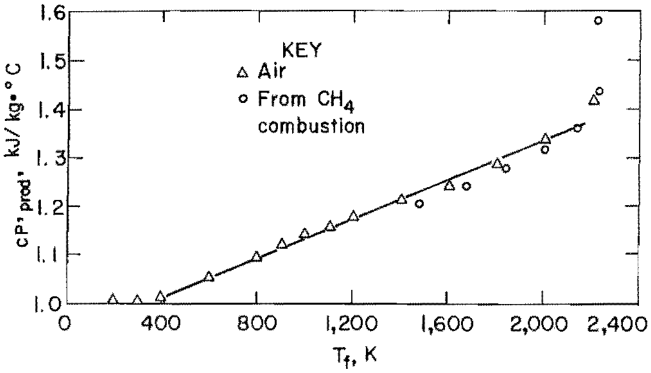

FIGURE A-2.–Effective specific heats of the combustion products of CH_4.

APPENDIX B.--CLOSED FORM SOLUTION OF EQUATION 8[1]

The roots for the following equation are desired: $\theta^4 + a_1(\theta-1) + a_2\theta(\theta-1) = a_3$.

This equation is of the form

$$\theta^4 + b\theta^2 + c\theta + d = 0, \qquad \text{(B-1)}$$

where

$$b = a_2,$$

$$c = a_1 - a_2,$$

$$d = -a_1 - a_3,$$

and it can be solved by Ferrari's method.

Equation B-1 is rearranged in the form

$$(\theta^2+\lambda)^2 - \{\theta^2(a\lambda-b) - c\theta+\lambda^2-d\} = 0, \qquad \text{(B-2)}$$

where λ is to be determined. The curly bracket becomes a perfect square if

$$c^2 - 4(2\lambda-b)(\lambda^2-d) = 0,$$

or

$$\lambda^3 - \frac{b}{2}\lambda^2 - d\lambda + \frac{bd}{2} - \frac{c^2}{8} = 0. \qquad \text{(B-3)}$$

To solve equation B-3, set $\lambda = y + b/6$, then

$$y^3 + py + q = 0, \qquad \text{(B-4)}$$

where

$$p = - d - \frac{b^2}{12},$$

and $$q = - \frac{b^3}{108} + \frac{bd}{3} - \frac{c^2}{8}.$$

[1]Equations without an alphabetic prefix, refer to equations in the main text.

Set

$$m = \sqrt[3]{- \frac{q}{2} + \sqrt{\frac{q^2}{4} + \frac{p^3}{27}}},$$

and

$$n = \sqrt[3]{- \frac{q}{2} + \sqrt{\frac{q^2}{4} + \frac{p^3}{27}}}.$$

Then the three roots of equation B-4 are

$$m + n, \quad wm + w^2n, \quad \text{and } w^2m + wn,$$

where

$$w = \frac{-1 + i\sqrt{3}}{2},$$

$$w^2 = \frac{-1 - i\sqrt{3}}{2}. \qquad \text{(B-5)}$$

The nature of the roots is determined from the discriminant

$$D = -4 \times 27 \left[\frac{q^2}{4} + \frac{p^3}{27} \right]. \qquad \text{(B-6)}$$

If $D < 0$, one real root and two conjugate complex roots.

$D = 0$, real equal roots.

$D > 0$, three real roots.

In this way, λ is determined by equation B-5. The curly bracket in equation B-2 is now a perfect square:

$$(\theta^2+\lambda)^2 - (2\lambda-b)\left\{\theta^2 - \frac{c}{2\lambda-b}\theta + \frac{\lambda^2-d}{2\lambda-b}\right\} = 0$$

or

$$(\theta^2+\lambda)^2 - (2\lambda-b)(\theta-\Omega)^2 = 0, \qquad \text{(B-7)}$$

which implies

$$\Omega = \frac{c}{2(2\lambda - b)}. \tag{B-8}$$

Equation B-7 now becomes

$$[\theta^2+\lambda + \sqrt{2\lambda-b}(\theta-\Omega)][\theta^2+\lambda - \sqrt{2\lambda-b}(\theta-\Omega)] = 0.$$

Hence,

$$\theta^2 + \sqrt{2\lambda-b}\ \theta + (\lambda-\Omega\ \sqrt{2\lambda-b}) = 0, \tag{B-9}$$

or

$$\theta^2 - \sqrt{2\lambda-b}\ \theta + (\lambda+\Omega\ \sqrt{2\lambda-b}) = 0. \tag{B-10}$$

From equation B-9

$$\theta = 1/2\left[-\sqrt{2\lambda-b} \pm \sqrt{-2\lambda-b + 4\Omega\ \sqrt{2\lambda-b}}\right], \tag{B-11}$$

and from equation B-10

$$\theta = 1/2\left[+\sqrt{2\lambda-b} \pm \sqrt{-2\lambda-b - 4\Omega\ \sqrt{2\lambda-b}}\right]. \tag{B-12}$$

Because real and positive roots are wanted, $\lambda = m + n$ from equation B-5 and θ is obtained from equation B-11 with the + sign for the square root.

APPENDIX C.--DERIVATION OF EQUATION 13[1]

The solution for equation 1 is known either for convection boundary conditions alone, or for radiative boundary conditions alone (constant q_r); a superposition technique can be applied. Set

$$T_t = T_1 + T_2, \tag{C-1}$$

where T_1 is the timber temperature when only the convective heat transfer exists, and T_2 is the temperature when only the radiative heat transfer exists. Equation 1 with the boundary and initial conditions of equations 2 through 4 yields the following two equations with different boundary and initial conditions, when equation C-1 is employed.

$$\frac{\partial T_1}{\partial t} = \alpha_t \frac{\partial^2 T_1}{\partial y^2} \tag{C-2}$$

Boundary conditions

$$\left.- \lambda_t \frac{\partial T_1}{\partial y}\right|_{y=0} = h_t (T_g - T_1) \qquad y = 0,\ t > 0$$

$$T_1 = T_\infty, \qquad y \to \infty,\ t > 0 \tag{C-3}$$

Initial conditions

$$T_1 = T_\infty, \qquad 0 \leqslant y < \infty,\ t = 0$$

$$\frac{\partial T_2}{\partial T} = \alpha_t \frac{\partial^2 T_2}{\partial y^2} \tag{C-4}$$

Boundary conditions

$$\left.- \lambda_t \frac{\partial T_2}{\partial y}\right|_{y=0} = - h_t T_2 + q''_{rad}$$

$$= h_t \left(\frac{q''_{rad}}{h_t} - T_2 \right), \qquad y = 0,\ t > 0$$

$$T_2 = 0, \qquad y \to \infty,\ t > 0 \tag{C-5}$$

Initial conditions

$$T_2 = 0, \qquad 0 \leqslant y < \infty,\ t = 0$$

---

[1] Equations without an alphabetic prefix refer to equations in the main text.

The solution for T_1 and T are (9, p. 106)[2]

$$\frac{T_1 - T_\infty}{T_g - T_\infty} = 1 - \mathrm{erf}\left(\frac{y}{2\sqrt{\alpha_t t}}\right) - \left[\exp\left(\frac{h_t y}{\lambda_t} + \frac{h_t 2\alpha_t t}{\lambda_t^2}\right)\right]$$

$$\left[1 - \mathrm{erf}\left(\frac{y}{2\sqrt{\alpha_t t}} + \frac{h_t\sqrt{\alpha_t t}}{\lambda_t}\right)\right], \quad \text{(C-6)}$$

$$\frac{T_2}{q''_{rad}/h_t} = 1 - \mathrm{erf}\left(\frac{y}{2\sqrt{\alpha_t t}}\right) - \exp\left[\left(\frac{h_t y}{\lambda_t} + \frac{h_t 2\alpha_t t}{\lambda_t^2}\right)\right]$$

$$\left[1 - \mathrm{erf}\left(\frac{y}{2\sqrt{\alpha_t t}} + \frac{h_t\sqrt{\alpha_t t}}{\lambda_t}\right)\right]. \quad \text{(C-7)}$$

The temperature at the timber surface (y = 0) is given as

$$T_{t,surface} = T_\infty + (T_g - T_\infty) + \frac{q''_{rad}}{h_t} G(t), \quad \text{(C-8)}$$

where

$$G(t) = 1 - \left[\exp\left(\frac{h_t 2\alpha_t t}{\lambda_t^2}\right)\right]\left[1 - \mathrm{erf}\left(\frac{h_t\sqrt{\alpha_t t}}{\lambda_t}\right)\right]$$

Equation C-8 is the desired equation, equation 13.

The total heat transfer to the timber, q''_{tot}, from t = 0 to t = τ_{ig} can be determined from

$$q''_{tot} = \int_0^{\tau_{ig}} \left[- \lambda_t \left.\frac{\partial T_t}{\partial y}\right|_{y=0}\right] dt$$

$$= h_t (T_g - T_\infty + q_r''/h_t) \int_0^{\tau_{ig}} \left[1 - \mathrm{erf}\frac{h_t\sqrt{\alpha_t t}}{\lambda_t}\right] \exp\left(\frac{h_t 2\alpha_t t}{\lambda_t^2}\right) dt. \quad \text{(C-9)}$$

A numerical integration is employed to evaluate q''_{tot}.

---

[2]Underlined numbers in parentheses refer to items in the list of references preceding appendix A.

APPENDIX D.--NUMERICAL SOLUTION FOR HEAT CONDUCTION EQUATION WITH CONVECTION AND RADIATION BOUNDARY CONDITIONS

The governing equations (1-4)[1] are cast into a finite difference scheme. An implicit scheme called Crank-Nicolson will be employed to assure stability in the numerical solution.

$$\frac{1}{2}\left[\frac{T^j_{i+1} - 2T^j_i + T^j_{i-1}}{(\Delta y)^2} + \frac{T^{j+1}_{i+1} - 2T^{j+1}_i + T^{j+1}_{i-1}}{(\Delta y)^2}\right] = \frac{1}{\alpha_t}\,\frac{T^{j+1}_i - T^j_i}{\Delta t} \qquad \text{(D-1)}$$

where T^j_{i+1} designates the temperature at grid point i + 1 at time j. If r is defined as

$$r = \frac{\alpha_t\ \Delta_t}{(\Delta y)^2}, \qquad \text{(D-2)}$$

equation D-1 becomes

$$-\,r\,T^{j+1}_{i-1} + (2 + 2r)\,T^{j+1}_i - r\,T^{j+1}_{i+1} = rT^j_{i-1} + (2 - 2r)\,T^j_i + rT^j_{i+1} \qquad \text{(D-3)}$$

Some simplification is achieved if r = 1,

$$-\,T^{j+1}_{i-1} + 4T^{j+1}_i - T^{j+1}_{i+1} = T^j_{i-1} + T^j_{i+1}. \qquad \text{(D-4)}$$

Equation D-4 applies to any interior point, i. At the boundary i = 1,

$$-T_L{}^{j+1} + 4\,T_1{}^{j+1} - T_2{}^{j+1} = T_L{}^j + T_2{}^j, \qquad \text{(D-5)}$$

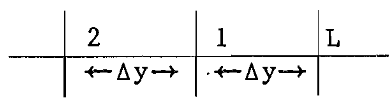

where i = L is a fictitious point just outside the boundary. The boundary condition, equation 2, can be written as, at time, j,

$$-\,\lambda_t\,\frac{T_2{}^j - T_L{}^j}{2\Delta y} = h_t\,(T_g - T_1{}^j) + P\varepsilon_t\sigma[T_g{}^4 - (T_1^j)^4].$$

---

[1]Equations without an alphabetic prefix refer to equations in the main text.

Solving for T_L^{J+1} gives

$$T_L^J = T_2^J + \frac{2h_f\Delta y}{\lambda_f}(T_g - T_1^J) + \frac{2P\varepsilon_f\sigma\Delta y}{\lambda_f}[T_g^4 - (T_1^J)^4]. \quad \text{(D-6)}$$

Similar expression for T_L^{J+1} can be written as

$$T_L^{J+1} = T_2^{J+1} + \frac{2h_f\Delta y}{\lambda_f}(T_g - T_1^{J+1}) + \frac{2P\varepsilon_f\sigma\Delta y}{\lambda_f}[T_g^4 - (T_1^{J+1})^4]. \quad \text{(D-7)}$$

Substituting equations D-6 and D-7 into equation D-5 yields

$$[2 + H_f + R_f\,(T_1^{J+1})^3]\,T_1^{J+1} - T_2^{J+1}$$

$$= -H_fT_1^J - R_f(T_1^J)^4 + T_2^J + 2H_fT_g + 2R_f\,T_g^4 \quad \text{(D-8)}$$

A set of finite difference equations consisting of equations D-8 and D-4 form a matrix of tridiagonal system. A standard solution technique is available for solving this system. A difficulty arises because of the coefficient term $[2 + H_f + R_f (T_1^{J+1})^3]$ in equation D-8, since T_1^{J+1} is unknown a priori. In the solution procedure, T_1^{J+1} is taken as the initial value for T_1^{J+1} and iterated until a convergence is attained.

The following computer program, FIRE.FOR, provides (1) the numerical solution as described in this appendix, and (2) the approximate solution, which is described following equation 13.

Control Parameters for FIRE.FOR

NCASE..... When NCASE = 3, no exact solution is computed.

L1........ When L1 = 0, no T_g calculation is performed.

IFLAG..... Number of time steps between printing. Note that DT * IFLAG is the actual time interval.

JFLAG..... JFLAG = 0 temp. distribution not printed. JFLAG = 1 temp. distribution printed.

IU........ Number of space steps between printing.

```
C  PROGRAM FIRE.FOR
      REAL L1,M1,N1, L2,M2,N2
      REAL LAMDA1, LAMDA2, LAMDAG, MUG
      COMMON TAU, SAI, BETA1, BETA2, H1,H2,L1,L2,M1,M2,N1,N2
      COMMON BRATIO,SAIL1,H,W
      DIMENSION FILEIN(3)
        DIMENSION U(500), COEF(500,3),RHS(500)
      IN=1
      IOUT=2
        OPEN(UNIT=IN,FILE='DFIRE.DAT',TYPE='OLD')
        OPEN(UNIT=IOUT,FILE='OTFIRE.DAT',TYPE='NEW')
C  IF NCASE = 3, NO EXACT SOLUTION COMPUTED.
      READ(IN,100) B,TOL,DELB, N,NDEL, NCASE
      READ(IN,102) TIMEI,TIMEF,DELT
      READ(IN,102) RHO1, LAMDA1, CP1
      READ(IN,102) RHO2, LAMDA2, CP2
      READ(IN,102) RHOG, LAMDAG, CPG
      READ(IN,108) H,W,L1,L2, ETA
      READ(IN,102) VINF, RHOINF, QF
      READ(IN,102) DELSAI,DELEND,EMIS
      READ(IN, 106) MUG, PR, HC, TIG
C  TEMPERATURES FOR REGION 2
C  FIRST CALCULATE THE NONDIMENSIONAL PARAMETERS
      ALFA1 = LAMDA1/(RHO1*CP1)
      ALFA2 = LAMDA2/(RHO2*CP2)
      BETA1 = ALFA1/ALFA2
      BETA2 = 1.0
        S1 = 2.0*(H + W)
        AREA = H*W
          DE = 4.*AREA/S1
        AMINF =RHOINF*AREA*VINF
        AMF = QF/HC
C  TO DETERMINE TC WHEN RADIATION IS CONSIDERED.
      IF(EMIS .EQ. 0.0) GO TO 3
        RDINO = 2.0*AREA*EMIS*5.669E-02*2.98**3
      RA1 = CPG*(AMINF + AMF)/RDINO
      RA2 = 0.0001961*298.0
      RA3 = QF/(RDINO*298.0)
        RB = RA1*RA2
        RC = RA1 - RB
        RD =  -RA1 - RA3
        RP = -RD - RB**2/12.0
        RQ = -RB**3/108. +RB*RD/3.0 - RC**2/8.0
        RBRA = SQRT(RQ**2/4.0 + RP**3/27.0)
      RM =  (RBRA -RQ/2.0)**(1./3.)
      RN = -(RBRA +RQ/2.0)**(1./3.)
        RY = RM + RN
      RLAMDA = RY + RB/6.0
        RFAC = 2.0*RLAMDA - RB
        ROMEGA = RC/(2.0*RFAC)
        RSQ = SQRT(RFAC-4.0*(RLAMDA-ROMEGA*SQRT(RFAC)))
      TNODIM =0.5*(-SQRT(RFAC) + RSQ)
      TC = 298.0*TNODIM
      GO TO 4
C  WHEN NO RADIATION IS CONSIDERED.
```

```
 3        CB0 = 1.0/(0.0001961*298.0)
          CB1 = CB0 - 1.0
          CB2 = CB0 + QF/(0.0001961*CPG*298.0**2*(AMF+AMINF))
        TNODIM = 0.5*(-CB1 + SQRT(CB1**2 + 4.0*CB2))
        TC = 298.0*TNODIM
 4        RHOG = 1.177*298.0/TC
          CPG = CPG*(1.0+0.0001961*(TC-298.0))
        VELG = (VINF*AREA*RHOINF + QF/HC)/(AREA*RHOG)
        VIEWFT =(VIEWF(L1+L2/3.)- VIEWF(L1))/(H*W)
            RED = RHOG*VELG*DE/MUG
          RQFLUX=H/L2*VIEWFT*EMIS*5.669*(TC/100.)**4
        COEFF1 =0.023*LAMDAG/DE*RED**0.8*PR**0.4
            REL2 = RHOG*VELG*L2/(6.0*MUG)
        COEFF2 = 0.102*(3.0/L2)*LAMDAG*REL2**0.675*PR**0.3333
          RATIO1 = RHO1*CP1/(RHOG*CPG)
          RATIO2 = RHO2*CP2/(RHOG*CPG)
        N1 = S1*COEFF1*L2**2*RATIO2/(AREA*LAMDA2)
        S2 = 2.0*H + W
        N2 = S2*COEFF2*L2**2*RATIO2/(AREA*LAMDA2)
        M2 = RHO2*CP2*L2*VELG/LAMDA2
        M1 = M2
        H1 = COEFF1*L2/LAMDA1
        H2 = COEFF2*L2/LAMDA2
           THEIG = (TIG-298.0)/(TC-298.0)
        WRITE(IOUT,152) RHO1, LAMDA1,CP1
        WRITE(IOUT,152) RHO2,LAMDA2,CP2
        WRITE(IOUT,152) RHOG,LAMDAG,CPG
        WRITE(IOUT,158) H,W,L1,L2
        WRITE(IOUT,162) ALFA1,ALFA2
        WRITE(IOUT,162) H1,H2
        WRITE(IOUT,162) M1,M2
        WRITE(IOUT,162) N1,N2
        WRITE(IOUT,164) COEFF1,COEFF2,VIEWFT
        WRITE(IOUT,555) TC,VELG,QF,THEIG,VINF,EMIS
        BRATIO = BETA2/BETA1
        SAIL1 = L1/L2
C * * * * * * * * * * * * * * * * * * * * * * * * * * * * * * - - - - -
C COMPUTATIONS START FROM HERE.
C FIX TAU AND CALCULATE TEMPERATURE AS FCN. OF SAI, TIME IN SECOND.
        TIME =TIMEI
           IF (L1 .EQ. 0.0) GO TO 41
     5 SAI = 0.0
        TAU = ALFA2*TIME/L2**2
    10 BP1= B
        ANS1 = SIMPS(0.0,BP1,N )
        BA1= B
        ANSA = SIMPSA(0.0,BA1, N, ETA)
    20 BP2= BP1+ DELB
        ANS2 = ANS1 + SIMPS(BP1,BP2,NDEL)
        ERROR = ABS(ANS1 - ANS2)
        ANS1 = ANS2
        BP1 = BP2
        IF (ERROR .GT. TOL) GO TO 20
    21 BA2= BA1+ DELB
        ANSB = ANSA + SIMPSA(BA1, BA2,NDEL, ETA)
```

```
      ERRORA = ABS(ANSA - ANSB)
      ANSA = ANSB
      BA1 = BA2
      IF (ERRORA .GT. TOL) GO TO 21
   23 THETAG =1.0-2.0/3.14159265*ANS2
      THETA = 1.0 - 2.0/3.14159265*ANSB
      QCVFLX = COEFF2*(TC - 298.)*(THETAG - THETA)
      WRITE(IOUT,550) TIME, TAU, SAI, BP2, BA2
      WRITE(IOUT,560) THETAG, ERROR, THETA,ETA,ERRORA
      WRITE (IOUT,570) RQFLUX, QCVFLX
      SAI = SAI + DELSAI
      IF (SAI .LE. DELEND) GO TO 10
      TIME = TIME + DELT
      IF (TIME .GT. TIMEF) GO TO 599
      GO TO 5
41    Y=COEFF2/LAMDA2*SQRT(ALFA2*TIME)
      G = 1.0 - EXP(Y**2)*(1.0-ERF(Y))
        T1 = 298.0 +(TC - 298.0)*G
        T2 = RQFLUX/COEFF2*G
        TT = T1 + T2
      THETA = (TT-298.0)/(TC-298.0)
      QCVFLX = COEFF2*(TC-TT)
      WRITE(IOUT,51) TIME,THETA,RQFLUX,QCVFLX
51    FORMAT(  5X, 'TIME =',F7.1, 'SEC', 5X,'THETA =',E13.5,5X,
     1 'RAD.FLUX =',E13.5,5X, 'CONV.FLUX =',E13.5)
      TIME = TIME + DELT
      IF (TIME .GT. TIMEF) GO TO 599
      GO TO 41
100   FORMAT(F10.0, E10.0, F10.0, 2I10, I2)
102   FORMAT(3F10.3)
104   FORMAT(2F10.2)
106   FORMAT(4E13.5)
108   FORMAT(5F10.3)
152   FORMAT(10X, 3F10.3)
158   FORMAT(10X, 4F10.3)
162   FORMAT(10X,2E13.5)
163   FORMAT(10X, 3E13.5)
164   FORMAT(8X,'COEFF1 =',E13.5,2X,'COEFF2 =',E13.5,2X,'VIEWFACTOR =',
     1 E13.5)
555   FORMAT( 7X, 'TC =',F7.1,2X, 'VELG =', F7.4,2X, 'QF =', E13.5,
     1  2X,'THETAIG =', E13.5, 2X,'VINF =',F7.4, 2X,'EMISSIVITY =',
     2  F7.4//)
550   FORMAT(  / 2X,'TIME =', F7.1, 'SEC', 2X, 'TAU =', E13.5, 2X,
     1 'SAI = ', E13.5, 2X,'BP =',F10.0, 2X,'BA =',F10.0)
560   FORMAT(10X, 'THETAG =', E13.5,2X, 'ERROR =',E13.5, 5X, 'THETA =',
     1 E13.5,2X, 'ETA =',E13.5,2X, 'ERROR = ',E13.5)
570   FORMAT(12X, 'RAD.FLUX =',E13.5,2X, 'CONV.FLUX = ',E13.5)
599     DELT1= TC/298.0 - 1.0
        ENUMB = QF/(AMINF*1005.*298.0)
        PARA1 = 2.0*EMIS*5.669E-08*AREA/(1005.*AMINF)
        PARA2 = AMF/AMINF
        ENERGY = QF*TIMEF
        WRITE(IOUT,171) DELT1, ENUMB, PARA1, PARA2, ENERGY
C  FOR GIVEN VINF,H,W,EMIS,AND TIND, WE CALCULATE THE CRITICAL CONDITIONS.
         FLO1 = RHOINF*VINF
```

```
 800      REL2 = FLO1*L2/(6.0*MUG)
          COEFF2=0.102*(3.0/L2)*LAMDAG*REL2**0.675*PR**0.3333
      YIND = COEFF2/LAMDA2*SQRT(ALFA2*TIMEF)
      GIND = 1.0 - EXP(YIND**2)*(1.0-ERF(YIND))
            C2 = H/L2*VIEWFT/COEFF2*EMIS*1.5002
          C3 = (TIG/298.0-1.0)/GIND + 1.0
      IF (EMIS .EQ. 0.0) GO TO 805
          A = 1.0/C2
          C = C3/C2
          SQ = (A**2)/16.0
          SQT = SQRT(SQ**2 + (C**3)/27.0)
          SM = (SQ + SQT)**(1./3.)
          SN = -(SQT-SQ)**(1./3.)
          SLAMDA = SM + SN
          SOMEG = A/(4.0*SLAMDA)
          STLAM = SQRT(2.0*SLAMDA)
      THETAG = 0.5*(-STLAM + SQRT(4.0*STLAM*SOMEG - 2.0*SLAMDA))
      GO TO 810
805   THETAG = C3
C  NEXT, DETERMINE AMFUEL.
      RDINO = 2.0*AREA*EMIS*5.669E-02*(2.98**3)
      RA2 = 0.0001961*298.0
810       RA4 = RDINO/1005.
          RA5 = (THETAG - 1.0)*(1.0 + RA2*THETAG)
          TOP = RA4*THETAG**4 + AMINF*RA5
          BOTTOM = HC/(1005.*298.0) - RA5
      AMFUEL = TOP/BOTTOM
          FLO2 = RHOINF*VINF + AMFUEL/AREA
          FLO3 = FLO1
          FLO1 = FLO2
          IF(ABS(FLO3-FLO1)/FLO3  .GT. 0.01) GO TO 800
      QF1 = AMFUEL*HC
      TG1 = 298.0*THETAG
         RQFLUX = EMIS*5.669*(TG1/100.0)**4
         QSURF = COEFF2*(TG1 + RQFLUX/COEFF2 - 298.)*SFCE(COEFF2,ALFA2,
     1    TIMEF,LAMDA2)
      WRITE (IOUT, 850) AMFUEL, TG1, QF1, QSURF
850   FORMAT(/10X, 'FUEL FLOW RATE =',E13.5,2X, 'TG1 = ',F7.1,2X,
     1 'QF1 = ',E13.5, 'QSURF =',E13.5)
171   FORMAT(//10X,'DELT/TINF =',F6.4,2X, 'ENUMBER =',F7.4,2X,
     1  'RAD. PARAMETER =',E13.5,2X, 'FLOW RATIO =', E13.5/10X,
     2  'ENERGY INPUT =', E13.5)
180      IF(NCASE .EQ. 3) GO TO 2500
C   THE FOLLOWING IS THE EXACT SOLUTION.
         READ (IN,3010) N,IFLAG,TOL1,DT,PP,EMIST,JFLAG,IU
         T=0.0
         TF=TIMEF
         DIF=ALFA2
         WRITE(IOUT,3015) N,IFLAG,TOL1,DT,PP,EMIST,JFLAG,IU
C  FIX INITIAL VALUES
         NP1=N+1
         DO 2010 I=1,NP1
         U(I)=298.0
2010     CONTINUE
         DX=SQRT(DIF*DT)
```

```
        IM=1
        QTT=0.0
        WRITE(IOUT,3020)
        HT=COEFF2*DX/LAMDA2
        RT=PP*EMIST*5.669E-08*DX/LAMDA2
C  ESTABLISH THE RHS VECTOR
2015    RHS(1)=2.0*RT*TC**4+2*HT*TC+U(2)-HT*U(1)-RT*U(1)**4
        DO 2020 I=2,N
        RHS(I)=U(I-1) + U(I+1)
2020    CONTINUE
C ESTABLISH COEFFICIENT MATRIX
2030    U1TRU=U(1)
        COEF(1,2)=2.+HT + RT*U(1)**3
        COEF(1,3)=-1.0
        DO 2035 I=2,N
        COEF(I,1)=-1.0
        COEF(I,2)=4.0
        COEF(I,3)=-1.0
2035    CONTINUE
C GET THE LU DECOMPOSITION TO PREPARE FOR SOLVING EQN.
2050    DO 2060 I=2,NP1
        COEF(I-1,3)=COEF(I-1,3)/COEF(I-1,2)
        COEF(I,2)=COEF(I,2)-COEF(I,1)*COEF(I-1,3)
2060    CONTINUE
C  GET THE SOLUTION
        U(1)=RHS(1)/COEF(1,2)
        DO 2070 I=2,N
        U(I)=(RHS(I)-COEF(I,1)*U(I-1))/COEF(I,2)
2070    CONTINUE
        DO 2080 I=1,N
        JROW=N-I+1
        U(JROW)=U(JROW)-COEF(JROW,3)*U(JROW+1)
2080    CONTINUE
        IF(ABS(U1TRU-U(1)) .GT. TOL1) GO TO 2030
        T = T+DT
        QC=COEFF2*(TC-U(1))
        QR=PP*EMIST*5.669*((TC/100.)**4 -(U(1)/100.)**4)
        QT=QC+QR
        QTT=QTT+QT*DT
        IF(IM .GE. IFLAG) GO TO 2090
        IM=IM+1
        IF(T .LT. TF) GO TO 2015
        GO TO 2500
2090    WRITE(IOUT,3030) T,U(1),QR,QC,QT,QTT
C PRINT OUT TEMP. DISTRIBUTION. JFLAG=0, NOT PRINT,JFLAG=1,
C  PRINT. IU IS THE NO. OF SPACE STEPS BETWEEN PRINTING.
        IF(JFLAG .LE. 0) GO TO 2095
        DO 4010 I=1,N,IU
                DEPTH=FLOAT(I-1)*DX
        WRITE(IOUT,4500) DEPTH,U(I)
4500    FORMAT(20X,'Y = ',E13.5, 5X,'T = ',E13.5)
4010    CONTINUE
2095    IM=1
        IF(T .LT. TF) GO TO 2015
3010    FORMAT(2I5,2E10.1,2F5.2,I2,I5)
```

```
3015     FORMAT(5X,2I5,2E15.3,2F10.2,'JFLAG=',I2,'IU=',I5)
3020     FORMAT(6X,'TIME',10X,'SURF.TEMP',5X,'RAD.FLUX',6X,'CONV.
    1FLUX',3X,'TOT.FLUX', 3X, 'TOT.HEAT IN'/)
3030     FORMAT(5X,F8.2, 5X, 5(E13.5,2X))
2500     STOP
      END
C   ******************************************************************
      FUNCTION SIMPS(AA, BB, NN)
      REAL L1,M1,N1, L2,M2,N2
      REAL LAMDA1, LAMDA2, LAMDAG
      COMMON TAU, SAI, BETA1, BETA2, H1,H2,L1,L2,M1,M2,N1,N2
      COMMON BRATIO,SAIL1,H,W
C   COMPUTE DELTA X.  ADD FIRST,SECOND,AND LAST VALUES TO SUM.
      SUM = 0.0
      NHALF = NN/2
      XN = FLOAT(NN)
      DELX = (BB-AA)/XN
      IF(AA .EQ. 0.0) GO TO 13
      SUM = FCN(AA) + 4.*FCN(AA+DELX) + FCN(BB)
      GO TO 14
   13 FIRST=N2*SAI/(M2*H2)+N1*SAIL1/(H1*M1)*SQRT(BRATIO)
      SUM =FIRST+ 4.*FCN(DELX) + FCN(BB)
C   ADD REST OF VALUES TO SUM
   14 X = 2.0*DELX
      Y = X + AA
      DO 15 I = 2, NHALF
      SUM = SUM + 2.*FCN(Y) + 4.*FCN(Y + DELX)
   15 Y = Y + 2.0*DELX
C   COMPUTE INTEGRAL AND OUTPUT THE VALUE.
      SIMPS= DELX/3.0*SUM
      RETURN
      END
C   * * * * * * * * * * * * * * * * * * * * * * * * * * * * * * * * * * *
      FUNCTION SIMPSA(AAA,BBB,NNN,YY)
      REAL L1,M1,N1, L2,M2,N2
      REAL LAMDA1, LAMDA2, LAMDAG
      COMMON TAU, SAI, BETA1, BETA2, H1,H2,L1,L2,M1,M2,N1,N2
      COMMON BRATIO,SAIL1,H,W
C   COMPUTE DELTA X.  ADD FIRST,SECOND,AND LAST VALUES TO SUM.
      SUM = 0.0
      NHALF = NNN/2
      XN = FLOAT(NNN)
      DELX = (BBB-AAA)/XN
      IF (AAA .EQ. 0.0) GO TO 23
      SUM = FUNC(AAA,YY) + 4.*FUNC(DELX+AAA,YY)+FUNC(BBB,YY)
      GO TO 24
   23 FIRS =N2*SAI/(M2*H2)+N1*SAIL1/(H1*M1)*SQRT(BRATIO)+YY+1.0/H2
      SUM = FIRS  + 4.*FUNC(DELX,YY) + FUNC(BBB,YY)
C   ADD REST OF VALUES TO SUM
   24 X = 2.0*DELX
      Y = AAA + X
      DO 25 I = 2, NHALF
      SUM = SUM + 2.*FUNC(Y,YY) + 4.*FUNC(Y+DELX, YY)
   25 Y = Y + 2.0*DELX
C   COMPUTE INTEGRAL AND OUTPUT THE VALUE.
```

```
      SIMPSA = DELX/3.0*SUM
      RETURN
      END
C * * * * * * * * * * * * * * * * * * * * * * * * * * * * * * * * * * * *
      FUNCTION FCN(SIG)
      REAL L1,M1,N1, L2,M2,N2
      REAL LAMDA1, LAMDA2, LAMDAG
      COMMON TAU, SAI, BETA1, BETA2, H1,H2,L1,L2,M1,M2,N1,N2
      COMMON BRATIO,SAIL1,H,W
        A1=N1/(H1**2+BRATIO*SIG**2)
        A2=N2/(H2**2+SIG**2)
        C1=H1*SAIL1*SIG/M1
         C2=H2*SAI*SIG/M2
        BRAKT1=(BETA1-A1)*BRATIO*SAIL1/M1*SIG**2
        BRAKT2=-TAU*BETA2*SIG**2+(BETA2-A2)*SAI/M2*SIG**2
        BRAKT3=A2*C2 + A1*SQRT(BRATIO)*C1
        FCN=1.0/SIG*EXP(BRAKT1 + BRAKT2)*SIN(BRAKT3)
      RETURN
      END
C * * * * * * * * * * * * * * * * * * * * * * * * * * * * * * * * * * * *
      FUNCTION FUNC(SIG,Y)
      REAL L1,M1,N1, L2,M2,N2
      REAL LAMDA1, LAMDA2, LAMDAG
      COMMON TAU, SAI, BETA1, BETA2, H1,H2,L1,L2,M1,M2,N1,N2
      COMMON BRATIO,SAIL1,H,W
        A1=N1/(H1**2+BRATIO*SIG**2)
        A2=N2/(H2**2+SIG**2)
        C1=H1*SAIL1*SIG/M1
         C2=H2*SAI*SIG/M2
        FACTR1=(BETA1-A1)*BRATIO*SAIL1/M1*SIG**2
        FACTR2=-TAU*BETA2*SIG**2+(BETA2-A2)*SAI/M2*SIG**2
        FACTR3=A2*C2 + A1*SQRT(BRATIO)*C1 +Y*SIG
      FUNC=1.0/(SIG*(H2**2+SIG**2))*EXP(FACTR1+FACTR2)*(H2**2
     1 *SIN(FACTR3)+H2*SIG*COS(FACTR3))
      RETURN
      END
C * * * * * * * * * * * * * * * * * * * * * * * * * * * * * *
      FUNCTION VIEWF(X)
      REAL L1,M1,N1, L2,M2,N2
      REAL LAMDA1, LAMDA2, LAMDAG, MUG
      COMMON TAU, SAI, BETA1, BETA2, H1,H2,L1,L2,M1,M2,N1,N2
      COMMON BRATIO,SAIL1,H,W
          IF(X.EQ.0.0) GO TO 300
        WHX=(W*W+H*H+X*X)**(H*H+X*X-W*W)
        WH=(W*W+H*H)**(H*H-W*W)
        WX=(W*W+X*X)**(X*X-W*W)
        HX=(H*H+X*X)**(H*H+X*X)
      VA=WHX*(H*H)**(H*H)*(X*X)**(X*X)/(WH*WX*HX*(W*W)**(W*W))
      VB=W*H*ATAN(W/H)
      VC=W*X*ATAN(W/X)
        HXSR=SQRT(H*H+X*X)
      VD=W*HXSR*ATAN(W/HXSR)
      VIEWF=1.0/3.1415926*(0.25*ALOG(VA)+VB+VC-VD)
          GO TO 310
300       VIEWF = 0.0
```

```
310   RETURN
      END
C  * * * * * * * * * * * * * * * * * * * * * * * * * * * * * * * * * * * *
      FUNCTION ERF(YZ)
      SUM = 0.0
      DELX = YZ/100.0
      SUM = 1.0+4.0*EXP(-DELX**2) + EXP(-YZ**2)
C  ADD REST OF VALUES TO SUM
      X = 2.0*DELX
      DO 65 I=2,50
      SUM = SUM + 2.0*EXP(-X**2) + 4.0*EXP( -(X+DELX)**2)
65    X = X + 2.0*DELX
C  COMPLETE INTEGRAL AND OUTPUT THE VALUE
      ERF = DELX/3.0*SUM*2.0/1.77245385
      RETURN
      END
C  ******************************
        FUNCTION SFCE(HT,ALFA,TIME,AMDA)
        SUM = 0.0
        DELX = TIME/100.
        SQRX = SQRT(DELX)
        P = HT/AMDA*SQRT(ALFA)
        P2 = P**2
        SUM =1.0+4.0*(1.0- ERF(P*SQRX))*EXP(P2*DELX) +
     1           (1.0- ERF(P*SQRT(TIME)))*EXP(P2*TIME)
C  ADD REST OF VALUE TO SUM
        X = 2.0*DELX
        DO  75 I = 2, 50
        SUM = SUM + 2.0*(1.0- ERF(P*SQRT(X)))*EXP(P2*X) + 4.0*(1.0-
     1           ERF(P*SQRT(X+DELX)))*EXP(P2*(X+DELX))
75      X = X + 2.0*DELX
C  COMPLETE INTEGRAL AND OUTPUT THE VALUE
        SFCE = DELX/3.0*SUM
        RETURN
        END
```

APPENDIX E.--ABBREVIATIONS AND SYMBOLS

A	cross-sectional area of duct
A_t	area of timber exposed to fire
C	constant
c_p	specific heat
E	source-fire parameter
H	duct height
ΔH	heat of reaction
h_t	heat transfer coefficient
L_t	length of a timber along axial direction of duct
ℓ	characteristic distance of heat transfer into solid
$\dot{m}$	constant
m	mass flow rate
n	constant
$P\varepsilon_t$	radiation transfer coefficient
Pr	Prandtl number = $c_{pg}\ \mu_g/\lambda_g$
$\dot{Q}_f$	heat release rate in source fire
q''	heat flux
R	radiative transfer parameter
T	temperature
ΔT	$T - T_\infty$
t	time

V	velocity
W	duct width
y	coordinate normal to timber surface
α	thermal diffusivity
β	temperature coefficient for specific heat
σ	Stefan-Boltzmann constant
ε	emissivity
λ	thermal conductivity
ρ	density
τ_{ig}	ignition time
μ	absolute viscosity

Subscripts

c	convective
f	fuel
g	combustion products
ig	ignition
net	net quantity
r	radiative
t	timber
tot	total quantity
∞	condition upstream of flame zone

U.S. GOVERNMENT PRINTING OFFICE: 1988 — 547-000/80,052

INT.-BU.OF MINES,PGH.,PA. 28728